DOI:10.14753/SE.2022.2759

CONTRIBUTION OF TITIN TO THE IMPROVED EXERCISE-INDUCED CARDIAC COMPLIANCE AND THE FUNCTIONAL EFFECTS OF DETRAINING IN THE RAT MODEL OF ATHLETE'S HEART

PhD Thesis

Dalma Lucia Kellermayer, MD

Doctoral School of Theoretical and Translational Medicine

Semmelweis University

Supervisor: Tamás Radovits, MD, PhD

Official reviewers: Attila Borbély, MD, PhD
Éva Ruisanchez, MD, PhD

Head of the Complex Examination Committee: István Karádi, MD, DSc

Members of the Complex Examination Committee: Péter Andréka, MD, DSc
Henriette Farkas, MD, PhD

Budapest
2022

DOI:10.14753/SE.2022.2759

Table of Contents

DOI:10.14753/SE.2022.2759

DOI:10.14753/SE.2022.2759

List of Abbreviations

A/C mode – resonant/non-contact mode of atomic force microscopy

AC – arrhythmogenic cardiomyopathy

AFM – atomic force microcsopy

Akt – protein kinase B

ATP – adenosine 5'-triphosphat

ATPase – adenosine 5'-triphosphatase

AV – atrioventricular

BDM – 2,3-butanedione-monoxime

BPM – beat per minute

BW – body weight

Ca^{2+} – calcium

CaMKIIδ – Ca^{2+}/calmodulin-dependent protein kinase IIδ

CCT – cardiac computed tomography

cGMP – cyclic guanosine monophosphate

CI – cardiac index

CMR – cardiac magnetic resonance imaging

CO – cardiac output

Co – control group

DCM – dilated cardiomyopathy

DCo – detrained control group

DEx – detrained exercised group

dP/dt_{max} – maximal slope of the systolic pressure increment

dP/dt_{max}-EDV – maximal slope of the systolic pressure increment and end-diastolic volume relationship

dP/dt_{min} – maximal slope of the diastolic pressure decrement

Ea – arterial elastance

ECG – electrocardiogram

ECM – extracellular matrix

EDPVR – end-diastolic pressure-volume relationship

EDV – end-diastolic volume

EF – ejection fraction

Eff – mechanical efficiency

ERK1/2 – extracellular signal-regulated kinase 1/2

ESPVR – end-systolic pressure-volume relationship

Ex – exercised group

FFM – fast force mapping mode of atomic force microscopy

FnIII – fibronectin type III domains

FS – fractional shortening

GCS – global circumferential strain

GLS – global longitudinal strain

GMWI – global myocardial work index

GRS – global radial strain

HCM – hypertrophic cardiomyopathy

HR – heart rate

HW – heart weight

Ig – immunoglobulin

IGF-1 – insluin-like growth factor 1

IGF-1R – insluin-like growth factor 1 receptor

IR – insulin receptor

IRS1 – insulin receptor substrate 1

IRS2 – insulin receptor substrate 2

JKR fitting mode – Johnson-Kendall-Roberts fitting mode

KO – knock-out

LA – left atrium

LV – left ventricle

LVEDD – LV end-disatolic diameter

LVEDP – left ventricular end-diastolic pressure

LVEDV – left ventricular end-diastolic volume

LVESP – left ventricular end-systolic pressure

LVESV – left ventricular end-sysstolic volume

MAP – mean arterial pressure

MHC – total myosin heavy chain

miR – microRNA

MLP – muscle LIM protein

mRNA – messenger ribonucleic acid

MW – myocardial work

MW – myocardial work

N2B – short cardiac titin isoform

N2B-us – N2B-unique sequence

N2BA – long cardiac titin isoform

Na^{+}/Ca^{2+} – sodium/calcium exchanger

P-V – pressure-volume

PEVK – region enriched in proline (P), glutamic acid (E), valine (V) and lysine (K) aminoacids

PI3K – phosphoinositide-3-kinase

PKA – protein kinase A

PKCα – protein kinase Cα

PKG – protein kinase G

PRSW – preload recruitable stroke work

PVA – pressure-volume area

RA – right atrium

RBM20 – RNA-Binding Motif 20

RNA – ribonucleic acid

RV – right ventricle

SCD – sudden cardiac death

SL – sarcomere length

STE – speckle tracking echocardiography

SV – stroke volume

SW – stroke work

T2 – proteolytic degradation product of titin

T3 – triiodthryonine

tau (τ) – time constant of left ventricular pressure decay

TK – serine-threonine protein kinase domain

TL – tibia length

TPR – total peripheral resistance

TR – thyroid hormone receptor

TRPC – transient receptor potential canonical channels

TT – total titin

TTN – titin gene

VAC – ventriculo-arterial coupling

VEGFB – vascular endothelial growth factor B

VEGFR – vascular endothelial growth factor receptor

1. Introduction

It has been widely investigated that regular physical activity has a beneficial effect on cardiovascular health (1-3). It has been shown, that life expectancy is moderately increased in physically active individuals (1, 3-5). Moreover, regular exercise reduces body weight and blood pressure, improves the plasma lipid profile and increases insulin sensitivity (1, 3). Many aspects of the effects of exercise have already been investigated. However, the morphological, functional and molecular cardiac adaptation to exercise is still not completely understood.

Furthermore, the functional effects of training reduction or detraining is not well characterized. Therefore, our aim was to characterize the effects of long-term physical exercise, including improved cardiac compliance, with a focus on the giant titin protein, and the functional role of detraining in the heart.

1.1. Athlete's heart in human and rodent studies

Long-term exercise induces complex cardiac remodeling, involving morphological and functional adaptation of the heart, referred to as athlete's heart (6-8). Athlete's heart is considered to be a physiological adaptation to exercise (7, 9-11). It is characterized by left ventricular (LV) hypertrophy, increased LV mass, wall thickness and enlarged cavities (6, 7). Previous studies showed that 1 hour exercise/day is sufficient to induce cardiac hpertyrophy (3, 8). Moreover, long-term exercise improves the contractility, relaxation and mechanoenergetic status of the heart (6-8, 12). However, professional athletes may achieve extreme levels of exercise and although it is accepted that training-induced LV hypertophy is a benign condition, there is emerging concern that it may be harmful in some cases (3, 13, 14).

Therefore, the evaluation of athlete's heart has undoubtedly become important for multiple reasons. It is crucial to explore the different molecular pathways of physiological and pathological cardiac hypertrophy to allow possible therapuetic targets for the diseased heart. Furthermore, high-quality morphological and functional measurements are fundamental to distinguish athlete's heart from pathological conditions and therefore possibly prevent sudden cardiac death (SCD) cases. In addition, studies of the athlete's heart contribute to our knowledge of physical performance in professional athletes.

Fortunately, to date, many researchers focus on the examination of ahtlete's heart in human studies and animal models.

1.1.1. Morphological changes in exercise-induced cardiac hypertrophy

Morganroth et al. were the first to describe morphological differences of the heart based on the type of exercise (15). It has been addressed that two main types of athlete's heart appear: endurance-trained and strength-trained heart (15-17) (Figure 1.). Cardiomyocytes are involved in the remodeling process induced by regular training (11, 16). Endurance sports (i.e. swimming, cycling, middle- and long-distance running) increase cardiac output and volume load on the ventricles, inducing a mild dilation of the ventricles (7, 18). Additionally, blood pressure is increased as well, resulting increased left ventricular wall thickness (7, 19). Therefore, in the myofibrils new sarcomeres are added *in-series* and the volume overload induces eccentric hypertrophy (16). On the other hand, strength training (i.e. weight lifting) elevates systolic and diastolic blood pressure, thus increases the afterload of the heart (20). The high intraventricular pressure results in increased myocardial wall stress, leading to concentric hypertrophy, in which sarcomeres are added *in-parallel* (16).

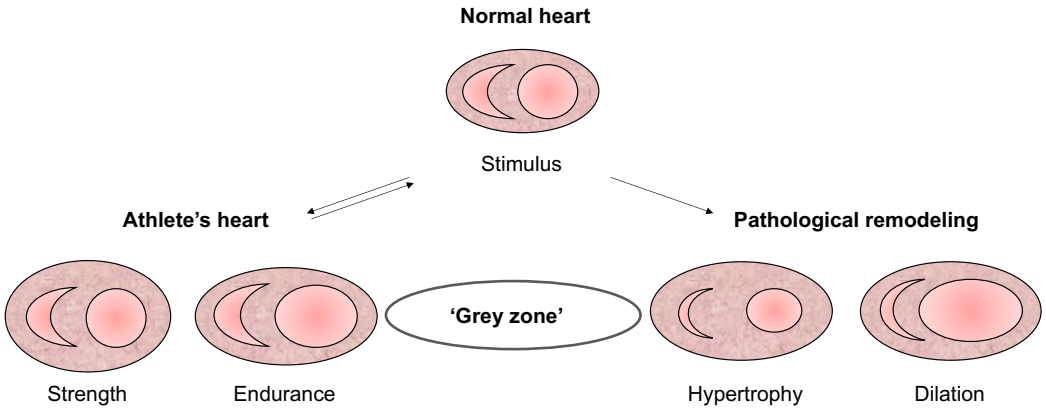

Figure 1. Schematic figure of physiological and pathological cardiac remodeling. Chronic exercise induces reversible physiological cardiac adaptation, termed athlete's heart. Up to 47% of the cases, athlete's heart morphology may fall into the 'grey zone' and overlaps with the characteristics of pathological conditions (21, 22). Therefore, it is truly important to distinguish the two phenotypes.

The gold-standard of the evaluation of athlete's heart dimensions is echocardiography. Over the past 40 years, numerous cross-sectional echocardiography studies have defined the cardiac morphology associated with long-term exercise (6, 7, 23, 24). The enlargement of the LV end-disatolic diameter (LVEDD) and the increased wall thickness appears in a wide range among athletes (6, 7). The main determining factors besides the type of sport are age, sex, race and body size (23). Endurance sports are the most likely to increase LV dimensions. Moreover, LVEDD could reach a maximum of 73 mm in professional cyclists (25). Animal studies of the athlete's heart also reported altered LV dimensions after long-term exercise (12, 26). Ethnic variations can also affect the chamber morphology in professional sportsman. Greater LV wall thickness (>12 mm) is present in Black athletes compared to White athletes (27). Even more, Black athletes can achieve ≥15 mm wall thickness with normal systolic and diastolic function. However, it is important to comprehensively evaluate these cases to differentiate athlete's heart from hypertrophic cardiomyopathy (HCM) (23, 27). Interestingly, gender differences were also seen in exercise-induced cardiac hypertrophy. Female athletes have lower LVEDD and wall thickness parameters than males. Although smaller cardiac dimensions were found in female rats, the propotional increment of the wall thickness was greater in females compared to males in the animal studies of athlete's heart (28-30). Most probably, the gender differences arise from the distinct molecular and hormonal pathways and further genetic factors (28, 31). Left atrial (LA) remodeling is also present in athlete's heart that is mainly related to LV enlaregement (7). The increased LA cavity is a benign phenomenon, however it is rarely associated with atrial fibrillation (7). Furthermore, the response of the right ventricle (RV) and right atrium (RA) is similar to that of the LV. The RV and RA dimensions are increased significantly, mainly in endurance-trained athletes (23, 32).

Besides echocardiography, cardiac magnetic resonance imaging (CMR) has become an essential imaging modality in the diagnostics of athlete's heart (21, 33-35). Moreover, cardiac computed tomography (CCT) may also be an additional method in the investigation of athlete's heart (35). Csecs et al. have reported sex differences in their evaluation of athletes with CMR (21). Males had larger ventricular volume and LV mass compared to females after long-term exercise (21). Moreover, male athletes demonstrated

higher LV and RV hypertrophy and concentric hypertrophy and LV cardiac remodeling was more common among professional male athletes (21). Importantly, a subset of these highly trained male athletes can fall into the "grey zone" and further assessment is required to distinguish exercise-induced LV hypertrophy from HCM (22) (Figure 1.).

1.1.2. Functional adaptation to exercise

In addition to the morphological and structural characterization of athlete's heart, it is certainly important to evaluate the functional consequences of exercise-induced cardiac hypertrophy.

LV function is primarily investigated by echocardiography. Ejection fraction (EF) and fractional shortening (FS) are the baseline systolic parameters to determine LV function. It has been described in echocardiographic and even with CMR studies that LV systolic function of highly-trained athletes is preserved or even slightly reduced EF and FS can be present at rest (36-40). On the contrary, in our previous study we showed increased EF and FS in a rat model after intense swimming exercise (12). Nevertheless, these parameters are highly dependent on HR, preload and afterload. Moreover, rats have higher HR values compared to humans that could explain the differences in these parameters. Although EF is the clinically most relevant value to estimate LV function, it does not describe the function precisely becuase of the aforementioned loading conditions (41). However, the recently developed speckle tracking echocardiography (STE) technique is able to characterize myocardial deformation, hence LV function, by the assessment of strain (longitudinal, radial, circumferential strain) and strain rate imaging (41, 42). Athletes demonstrate normal, higher or even slightly reduced global longitudinal strain (GLS) (43). This disparity is a possible consequence of the variety in LV geometry induced by different training types. No major differences were reported in global circumferential strain (GCS) and global radial strain (GRS) between athletes and controls (43). On the contrary, Kovács et al. demonstrated significantly improved GLS and GCS in exercised rats compared to that of controls (44). Nonetheless, GLS is also influenced by HR and loading conditions. Therefore, myocardial work (MW) might be able to assess LV function more precisely than GLS in a noninvasive manner, independently from loading conditions (45). A recent study of Tokodi et al. reported significantly improved

global myocardial work index (GMWI) in exercised rats and highly trained athletes (45). Furthermore, GMWI reflected the supernormal LV function of athlete's heart at rest (45).

Interestingly, it has been revealed that LV diastolic function is often supernormal in athletes. (2, 25, 37, 46, 47). Moreover, myocardial stiffness is reduced in athlete's heart (48, 49). Therefore, exercise-induced LV hypertrophy is associated with improved diastolic function and hence cardiac compliance (48, 49). The ratio of early (E) and late/atrial (A) LV filling by using tissue Doppler echocardiography is normal or slightly enhanced in athletes, also confirming improved diastolic function in highly trained athletes (42). Increased LV untwisting rate was revealed in exercised hearts that could also enhance early diastolic suction (37, 50). Moreover, Lakatos et al. reported that pronounced LA dilation and lower resting functional parameters are associated with improved exercise performance (51). Although there are conflicting data about the RV remodeling to exercise, it has been identified that the RV diastolic function is enhanced in endurance-trained athletes (32).

Nevertheless, the aforementioned noninvasive imaging approaches are highly dependent on loading conditions. Therefore, in the past decade research groups utilized sensitive miniature pressure-volume (P-V) catheters in small animal models to evaluate *in vivo* cardiac function independently of loading conditions (12, 28, 52, 53). The slope of end-systolic pressure-volume relationship (ESPVR), preload recruitable stroke work (PRSW) and the maximal slope of the systolic pressure increment and end-diastolic volume relationship (dP/dt_{max}-EDV) are sensitive indices that describe the ventricular contractility of the heart *in vivo* (52, 54). In a previous study of our research group, P-V analysis has revealed improved contractility, haemodynamic conditions and enhanced active relaxation in exercised rats (12). Moreover, research on experimental animals contributed to our knowledge of the mechanoenergetic status of the heart after long-term exercise. The myocardial energetics parameters pressure-volume area (PVA), ventriculo-arterial coupling (VAC), stroke work (SW) and efficacy were also ameliorated in trained animals (12, 28) after 12 weeks of swim training.

The cellular mechanism underlying the functional improvement of exercise-induced LV hypertrophy has been under extensive discussion. Functional studies on mouse and rat cardiac trabecular muscles and cardiomyocytes have revealed increased Ca^{2+} sensitivity, improved rate of force production and loaded shortening velocities in trained

animals (55-59). Training-induced Ca^{2+} sensitivity only occurs at higher sarcomere lengths. This potentially explains why exercise increases left ventricular function at higher EDV (55, 56). Further studies revealed increased activity of the sodium/calcium (Na^{+}/Ca^{2+}) exchanger (60) and the Ca^{2+} ATPase of the sarcolemma and the sarcoplasmatic reticulum (61, 62). Moreover, exercise also affects the stiffness of the cardiac muscle. Slater et al. reported reduced passive stiffness in LV wall strips of mice after 3 weeks of voluntary wheel running (63).

1.1.3. Electrical changes of the heart after long-term exercise

Long-term exercise also induces electrical changes of the heart detected on electrocardiogram (ECG) (64). The ECG alterations are dependent from race, age, sex and the type and intensity of exercise (64). Athletes frequently have increased vagal tone associated with sinus bradycardia and atrioventricular (AV) conduction block. Sinus bradycardia (lowest accepted normal heart rate is 30 beats per minute (BPM)), Mobitz I AV block, junctional rhythm and incomplete right bundle branch block are considered normal in athletes (64-66). Further ECG alterations have been determined in 'The International Recommendations for the Interpretation of the ECG in the Athlete', including signs of early repolarisation and voltage criteria for LV hypertrophy (64). In cases of abnormal ECG patterns, further prompt and extensive evaluations must be taken (64, 66, 67).

1.1.4. Molecular alterations involved in exercise-induced LV hypertrophy

Exercise-induced cardiac hypertrophy is triggered by various hypertrophic stimuli at the cardiomyocyte level (68). There are two main initiating trigger pathways to induce physiological LV hypertrophy: biochemical signals and strech-sensitive mechanisms (68, 69).

The initiating signals of triiodthryonine (T3), vascular endothelial growth factor B (VEGFB), insluin and insulin-like growth factor 1 (IGF-1) are the main molecules participating in the induction of physiological cardiac hypertrophy. The most crucial and recognized signaling pathway is the IGF-1 activated PI3K (phosphoinositide-3-kinase) - Akt cascade (68-73). IGF-1 binds to the IGF-1 receptor (IGF-1R), a transmembrane tyrosine kinase receptor, that subsequently activates the PI3K-Akt signaling cascade (68,

69). The cardioprotective p110α subunit of PI3K is the key regulator of physiological hypertrophy (69, 71). Moreover, Akt also has a critical role in physiological LV growth, as Akt-defitient mice have impaired cardiac response to exercise (72, 74). Moreover, insulin binds to the tyrosine kinase insulin receptor (IR) followed by the phosphorylation of insulin receptor substrate 1 (IRS1) and IRS2 which also activates the PI3K-Akt pathway. The insulin mediated signaling pathway plays an essential role in postnatal physiological cardiac growth. Heart specific deletion of IRs have resulted smaller hearts and reduced cardiomyocyte number in mice (68). The additional activation of VEGF receptors (VEGFR) and thyroid hormone receptors (TR) also regulate gene activation, protein synthesis and metabolic pathways that are involved in the mechanism of physiological LV hypertrophy (68).

Mechanosensors also play a fundamental role in the induction of exercise-induced LV hypertrophy (68). Special mechonsening proteins convert mechanical forces into biochemical signals that initiate cardiac growth. Myocardial stretch activates transient receptor potential canonical channels (TRPC) leading to Ca^{2+} influx and the activation of prohypertrophic signaling pathways (68). Integrins mediate mechanotransduction by sensing changes in the extracellular matrix (ECM) (68). The sarcomeric Z-disk, anchoring actin filament, encompasses multiple mechanosensing structural proteins as muscle LIM protein (MLP), telethonin, obscurin and titin that also regulate myocardial hypertrophy (68, 75). Furthermore, titin not only plays a role in hypertrophic signaling pathways but also cotributes to myocardial mechanics (76).

1.2. Titin, the regulator of cardiac compliance

1.2.1. The structure and function of striated muscles

Striated muscle is comprised of two types of tissue: skeletal and cardiac muscle (77, 78). Striated muscle contracts and generates force to support locomotion, posture and breathing with skeletal muscle and to provide blood circulation with cardiac muscle (77, 79). Striated muscle is composed of myofibers, that are consisted of myofibrils (79, 80). The myofibrils contain repeating sections of sarcomeres (81, 82) (Fig. 2.). The sarcomere is the functional unit of the muscle cell, that is composed of long myofilament proteins (82, 83). The two main myofilament types are the thick (mainly formed by myosin) and thin filaments (primarily actin) (77, 83). Furthermore, titin is the third most abundant

myofilament of the contractile unit (84-87). During contraction, myosin heads bind to actin and by the hydrolysis of adenosine triphosphate (ATP), myosin initiates a power stroke and slides the actin filament inwards, thereby shortening the sarcomere and generating active muscle force (88, 89). At higher sarcomere lengths, striated muscle develops passive tension, that is added to the total force (77, 90). Passive tension in cardiac muscle is predominantly determined by titin (91). Titin-based passive tension also contributes to length-dependent force production, as known as the Frank-Starling law in cardiac muscle (53, 92).

The sarcomere displays a striated pattern, first described by Van Leeuwenhoek (93, 94). The sarcomere length is determined by the neighbouring Z-disks. The physiological slack length (resting sarcomere length) is 1.7-2.2 μm in the cardiac muscle (95). The Z-disk anchors actin and appears as a dark line on electron micrographs. The I-band (isotropic) surrounds the Z-disk and contains actin. It is followed by the A-band (anisotropic), containing both actin and myosin. The I- and A-bands are named after their properties under polarized light microscope. The H-zone is localized at the end of the A-band that involves myosin. The M-band is the middle of the sarcomere and appears within the H-zone. Several proteins of the cytoskeleton apparatus are embedded in the M-band (77, 82).

1.2.2. The elastic myofilament, titin

The main regulator of cardiac compliance is the giant elastic protein, titin (49, 91). Titin spans half of the sarcomere, therefore it is extended from the Z-disk to the M-line (84, 85) (Figure 2.). It is encoded by the *TTN* gene and contains 363 coding exons (96). It is composed of immunoglobulin (Ig) and fibronectin type III (FnIII) domains and unique sequences (85, 97). Titin is expressed in cardiac and skeletal muscle (85, 96). Its main role is to provide passive stiffness to striated muscle (91, 98, 99). Moreover, it also modulates active contractile force (53, 100, 101).

The NH2-terminus of titin, embedded in the Z-disk, acts as a mechanosensor (75). Titin's I-band region serves as a molecular spring and determines elasticity in cardiomyocytes (91). It comprises tandem Ig domains and unique sequences as the N2B-unique sequence (N2B-us) and the PEVK region enriched in proline (P), glutamic acid (E), valine (V) and lysine (K) aminoacids (85, 96). It has been suggested that these

segments also function as mechanosensor complexes as they interact with numerous signaling proteins (102, 103). The A-band region of titin contains the I/A zone, the D-zone and the C-zone and is functionally inextensible (85, 97, 104). The C-zone segment plays a part in the regulation of the actomyosin interaction and thick filament regulation (104). Titin's COOH-terminus is anchored in the M-line (85, 96). The M-band segment of titin contains the serine-threonine protein kinase (TK) domain and has a pivotal role in multiple signaling pathways (102, 103, 105).

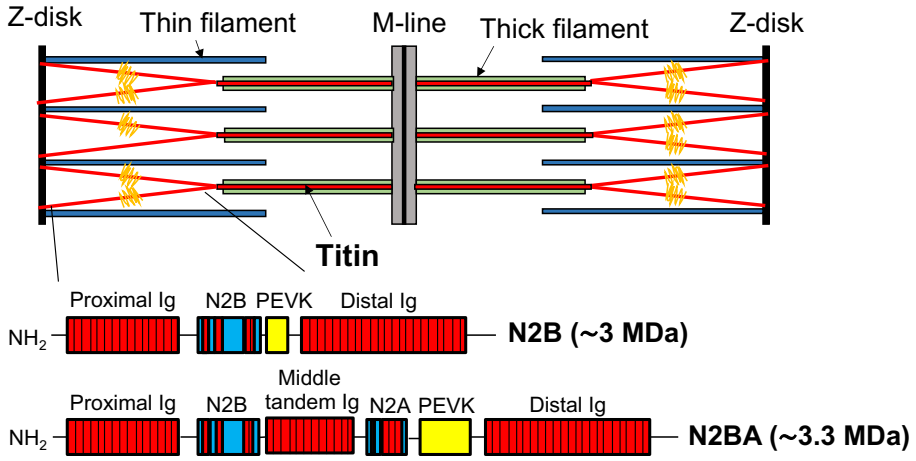

Figure 2. Schematic representation of the sarcomere structure and adult cardiac titin isoforms.

1.2.3. Titin isoforms

Titin's spring region undergoes extensive alternative mRNA splicing regulated by the RNA-Binding Motif 20 (RBM20), resulting in distinct titin isoforms (106). The isoforms differ in the length of the tandem Ig and PEVK segments (96, 106).

The adult cardiac titin contains two main titin isoforms: the longer, more compliant N2BA (~3.3 MDa) and the shorter and stiffer N2B (~3 MDa) titin (85, 96, 99) (Figure 2.). These isoforms are co-expressed with an expression ratio (N2BA:N2B) of ~0.5 in normal human hearts (107). However, the ratio varies in different species (108) and disease states (107, 109, 110).

Besides full-length titins, shorter titin isoforms are also present. Novex-3 (~700 kDa) contains a polyadenylation stop codon signal resulting in a truncated titin that acts as an alternative C-terminus (96, 111). It has been recently discovered that TTN also contains an alternative start signal that expresses Cronos titin (~2 MDa) (112). Cronos lacks the

Z-disk and most of the I-band segments but contains the A- and M-band region (112). Nevertheless, the exact function of Novex-3 and Cronos titin is yet to be identified.

Titin is also a substrate of calpain cleavage that severs titin's connection to the Z-disk (113). Titin is cleaved in the I-band region into a ~2 MDa fragment, known as the T2 proteolytic degradation product, and into a ~1.2 MDa fragment (114). The latter is unstable and is quickly degraded into smaller fragments (113). T2 is similar to Cronos titin and contains the A-band and M-line segments of titin and part of the I-band region (114).

1.2.4. Modulation of passive stiffness in cardiomyocytes induced by exercise

Titin is the main regulator of myocardial stiffness (49, 91). Alterations in titin-based passive stiffness affect the wall tension of the ventricles and thus affect the diastolic filling (49). Subsequently, the systolic function of the heart is modified via the Frank-Starling mechanism (49, 53, 100). Moreover, reduced passive stiffness is associated with increased exercise tolerance (49). In addition, exercise itself could induce short- and long-term alterations in titin-based passive stiffness. Passive stiffness, hence elasticity and compliance can be modified via post-translational modifications on the spring elements of titin or via alterations in the expression of titin isoforms (49, 115).

Phosphorylation is the most extensively evaluated post-translational modification of titin (115). Titin has multiple phosphorylation sites, of which a few outstanding phosphosites have been characterized in details (63, 115-118). The altered phosphorylation of titin has been analyzed in the N2B-us and PEVK region, as these segments are mechanically active elements of the I-band (63, 116-119). There is a consensus that titin-based passive stiffness is reduced by N2B-us phosphorylation (114, 118-122), whereas phosphorylation of the PEVK element increases stiffness (63, 116). There are five main kinases that can phosphorylate the spring region of titin: protein kinase A (PKA), protein kinase Cα (PKCα), cyclic guanosine monophosphate (cGMP) dependent protein kinase G (PKG), extracellular signal-regulated kinase 1/2 (ERK1/2), and Ca^{2+}/calmodulin-dependent protein kinase IIδ (CaMKIIδ) (115, 123). Ser4010, targeted by PKA and ERK1/2 and Ser4099, targeted by PKG are localized in the N2B-us (117, 118, 124). In the PEVK region Ser11878 and Ser12022, targeted by PKCα and CaMKIIδ are the most investigated phosphosites (116, 119). Previous studies focused on

post-translational phosphorylation modifications after 15 min treadmill running or 3-6 weeks voluntary wheel running in rodent models (63, 117, 125).

Recent studies focused on oxidation as another possible post-translational mechanism to modify titin-based stiffness including disulfide bonding in the N2B-us and Ig domains and S-glutathionylation of the Ig domains (115, 126, 127). Nevertheless, currently there is no data on titin oxidation after exercise.

Post-translational modifications represent short-term mechanisms to modify titin-based stiffness (115). However, titin isoform switching provides an important long-term mechanism to alter passive stiffness (49, 115).

Increased expression of the more compliant N2BA titin isoform, thus elevated N2BA/N2B ratio reduces passive stiffness that corresponds to a more compliant heart (99, 110). Although titin isoform switch occurs during the perinatal period (99, 128, 129) or in pathological states (109, 110), limited data is available on titin isoform alterations after long-term exercise. An exercise-induced titin isoform change has been shown in a titin Ig knock-out (KO) mouse model (130). A recent study by Chung et al. revealed increased N2BA expression in trained rats (131). However, it should be stressed that previous research groups utilized voluntary wheel running that could induce different adaptations compared to controlled high-intensity training protocols (i.e. swimming, treadmill running) (63, 117, 130, 131). Moreover, no previous investigations have been conducted to evalute the impact of titin alterations on the cardiac sarcomere structure and mechanics after long-term high intensity exercise.

1.2.5. Atomic force microscopy (AFM) imaging

Atomic force microscopy is a powerful imaging modality that allows the visualization and manipulation of native biological samples at (sub)nanometer resolution (132-134). An AFM can operate in static (contact) or dynamic (resonant, non-contact/“tapping”) modes (132, 133) (Figure 3.). In the resonant AFM, the sample is scanned with a sharp tip attached to the end of a flexible cantilever (133, 135). During scanning, the tip becomes close to the sample resulting the oscillation of the cantilever. The oscillation of the cantilever is detected through the deflection of a laser beam that is reflected from the cantilever (133, 135) (Figure 3.).

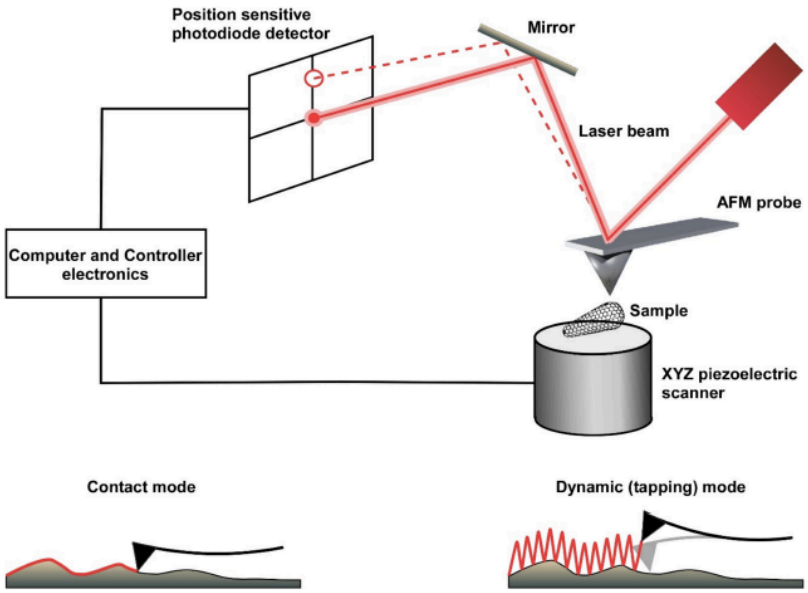

Figure 3. Schematic image of the AFM components. The dynamic mode is a powerful method to scan soft biological samples. The image is adapted from the work of Rousso and Deshpande (136).

The fast force mapping (FFM or jumping mode) of the AFM allows force spectroscopy and transverse elasticity measurements (133, 137, 138). In FFM the cantilever is driven sinusoidally and each pixel corresponds to a force curve (137). The Young's modulus, describing the elasticity against compressive forces, is obtained by different fitting models on the force curves (139). Therefore, AFM is an appropiate platform for the high-resolution evaluation of single molecules or cells, even myofilaments or myofibrils (134, 140, 141).

1.3. Effects of detraining

1.3.1. Regression of training-induced morphological and functional cardiac adaptation

Athlete's heart is considered as a reversible physiological condition. However, the regression of the morphological and functional cardiac features are still under review (7, 142). Training termination or detraining may regress exercise-induced cardiac adaptations towards a more normal structure (10, 143-146). Significant reduction in LV cavity dimensions and wall thickness in former professional athletes was seen after long-

term detraining (7, 10, 147-149). Swoboda et al. reported reduction in LV mass after 1 month of complete deconditioning (11). Based on CMR measurements, they demonstrated decreased intracellular myocardial compartment (primarily cardiomyocytes) with no alterations in the extracellular compartment (11).

A few evaluations on experimental animals revealed regression of training-induced cardiac morphological changes after deconditioning (13, 62, 150). Experiments on isolated cardiomyocytes and intact papillary muscles from rats suggested functional reversibility after the cessation of training (13, 62, 150). Benito et al. revealed collagen deposition in the RV of trained rats accompanied by diastolic dyfunction (13). However, the impaired cardiac remodeling parameters reversed to control levels after 8 weeks of detraining (13). Additionally, load-dependent echocardiographic measurements provided data on the possible reversibility of functional parameters of the exercise-induced cardiac adaptation in top-level athletes (10). Furthermore, although no systolic dysfunction or wall motion abnormality was detected in either athlete after deconditioning, LV chamber dilation was still observed in a few cases (10, 151). However, the functional effects of detraining in the intact heart needs to be further evaluated. Therefore, additional investigations are required to determine whether the residual LV hypertrophy has long-term clinical implications.

1.3.2. Role of detraining in the 'grey zone'

The cessation of exercise is also a commonly used, helpful test to distinguish athlete's heart from pathological conditions (10, 11, 152). Modestly increased LV wall thickness (13-15 mm) has been observed in ~ 2% of the adult male professional athletes that falls into the so called 'grey zone' (7). The grey zone defines the overlap between the morphology of athlete's heart (e.g. extreme hypertrophy, enlarged LV cavity, ECG alterations) and the features of pathological conditions, as hypertrophic cardiomyopathy (HCM), dilated cardiomyopathy (DCM) or arrhythmogenic cardiomyopathy (AC) (7, 153, 154). However, Czimbalmos et al. reported that even 47% of their study population reached the cut off point of the grey zone (22). Interestingly, only 4% of the female athletes fell in the grey zone, demonstrating gender differences in the morphology of athlete's heart (22). A typical of 1-3 months long period is required to evaluate the regression of LV hypertrophy in these cases (11, 142, 148). Nevertheless, the compliance

with deconditioning is often poor among athletes (11). Therefore, it is important to acquire high-resolution imaging modalities (i.e. CMR) (11, 22, 35, 155) and consider additional genetic testing for differential diagnosis before training reduction is applied (7, 23).

1.3.3. Sudden cardiac death (SCD)

There is increasing concern that high-intensity exercise is possibly associated with malignant ventricular arrhythmias or sudden cardiac death (SCD) (3, 4, 7, 156). Therefore, training-induced LV hypertrophy could be potentially harmful in some individuals. The most common causes of SCD in young athletes (age <35 years) are congenital or inherited diseases, predominantly HCM (3, 157). Interestingly, an Italian registry demonstrated AC as the most common cause of sudden cardiac arrests (3, 158). Nevertheless, normal heart structure was found in 3% of the SCD cases (157).

Overall, exercise-induced cardiac hypertrophy should be investigated by physicians with experience in sports medicine. Furthermore, careful evaluation of the effects of long-term training and deconditioning on the heart's morphology and function is obligatory in human athletes and experimental animal models.

1.4. Animal models of exercise-induced left ventricular hypertrophy and detraining

In humans, physiological cardiac hypertrophy is investigated by non-invasive methods (i.e. echocardiography, CMR, CT) (6, 35) with the exception of a few invasive P-V measurements, mainly in heart failure patients (54). In order to evaluate the functional and molecular biology of training-induced LV hypertrophy, it is fundamental to rely on experimental animal models. Numerous types of training protocols have been established in different laboratory animals to investigate athlete's heart (159).

1.4.1. Small animal models (mouse, rat)

Rodent animal models are suitable for a wide range of experiments (159). They have a short gestation period with high numbers of offsprings. Moreover, they reach young adult age within 2-3 months (160). Genetic engineering is also more available in small animal models (161).

Voluntary wheel running

Voluntary wheel running is an easy method to examine LV hypertrophy (29, 63, 117). However, it has a limiting factor, since it relies on the animal's effort level (162). Nevertheless, previous studies reported 10-15 km/day voluntary running for 2-4 weeks that was able to induce robust LV hypertrophy in rats (162). It is important to note that the motivation declined after 4 weeks (159, 162). Overall, voluntary wheel running is an accepted training protocol for the evaluation of exercise-induced LV hypertrophy.

Treadmill

Treadmill running allows many training protocols with different session duration, speed and inclination (163, 164). In general, the exercise protocol lasts from weeks to months. Furthermore, treadmill running also provides the possibility of interval training investigations (159).

Swim training

Swimming is another possible training method to evaluate physiological LV hypertrophy (12, 159, 165). The animals are placed in water tanks, separately. Usually 1-6 h/day for 1-24 months training periods are applied. The exercise load could be modulated by attaching tail weight or floating devices to the animals. The water temperature may also influence the development of LV hypertrophy. 30-36 °C was considered to equally induce cardiac hypertrophy in young and aged animals (159).

1.4.2. Large animal models

Larger animal models may represent the human heart more accurately than small rodents (160). However, they are more costly and require more management. Even more, the gestation period is longer and genetic models are limited (159). Nevertheless, previous studies successfully used swine, dog and rabbit treadmill training models to investigate LV hypertrophy induced by exercise (159, 166, 167).

DOI:10.14753/SE.2022.2759

2. Objectives

Athlete's heart, the functional and morphological cardiac adaptation to long-term exercise, has become the point of interest of sports cardiology in the past decades. Although many aspects of athlete's heart have been evaluated, no data are available on the modifications of sarcomere morphology and mechanics due to titin alterations after long-term exercise. Moreover, we have limited knowledge of the effect of detraining on left ventricular (LV) function.

The purpose and aims of the present study were:

1) Evaluation of titin's role in the improved cardiac compliance of exercise-induced left ventricular hypertrophy
    i) Induction of athlete's heart by a 12-week-long swim training protocol in a rat model. Assessment of LV hypertrophy by echocardiography and tissue weights.
    ii) Examine total titin content, titin isoform expression and post-translational phosphorylation of titin of the left ventricle by using molecular biological methods.
    iii) Determine whether any training-induced titin modification has an impact on the sarcomere structure and elasticity of single myofibrils isolated from the left ventricle by atomic force microscopy.

2) Investigate the effects of detraining on left ventricular performance
    i) Evaluate the morphological reversibility of exercise-induced LV hypertrophy by echocardiography, tissue weights and histology after an 8-week-long detraining period.
    ii) Provide detailed characterization of *in vivo* LV haemodynamic alterations (contractility, relaxation, stiffness, cardiac energetics) after the cessation of exercise by LV pressure-volume (P-V) analysis.

3. Results

3.1. Exercise-induced cardiac hypertrophy

All of the animal experimental procedures were approved by the Ethical Committee of Hungary for Animal Experimentation (License number: PEI/001/2374-4/2015) in accordance with the 'Principles of Laboratory Animal Care' defined by the National Society for Medical Research and the Guide for the Care and Use of Laboratory Animals, provided by the Institute of Laboratory Animal Resources and published by the National Institutes of Health (publication no. 85-23, revised 1996) and the European Union Directive 2010/63/EU.

Cardiac hypertrophy was observed by echocardiography in the exercised (DEx) group after 12 weeks of swimming compared to control (DCo) rats. (Figure. 4A). Left ventricular wall dimensions (anterior and posterior wall thickness) were significantly increased in trained rats. Moreover, LV mass and LV mass index increased significantly after the 12-week-long swimming period. Furthermore, the heart weight, heart weight-to-body weight ratio (HW/BW) and HW to tibia length (HW/TL) ratio increased significantly in exercised (Ex) rats in comparison to the control (Co) group (Table 1.). There was a trend of reduced BW in the Ex group, but it did not reach the significant level. These results indicate the development of cardiac hypertrophy and thus athlete's heart. Echocardiographic measurements showed improvement of the systolic function of the exercised hearts; ejection fraction (EF) and fractional shortening (FS) improved significantly after training (Figure 4A).

Table 1. Body and heart weight data.

The exercised group has significantly increased heart weight data. The body weight did not reduce significantly in the exercised rats. Data are expressed as mean ± SEM. BW: body weight, TL: tibia length, HW: heart weight, HW/BW: heart weight to body weight ratio, HW/TL: heart weight to tibia length ratio. *$p < 0.05$

DOI:10.14753/SE.2022.2759

	Co (n=6)	Ex (n=6)	p-value
BW (g)	483 ± 24	417 ± 18	0.06
TL (cm)	4.33 ± 0.05	4.18 ± 0.06	0.09
HW (g)	1.23 ± 0.05	1.45 ± 0.08*	0.04
HW/BW (g/kg)	2.55 ± 0.08	3.47 ± 0.09*	<0.01
HW/TL (g/cm)	0.28 ± 0.01	0.34 ± 0.01*	<0.01

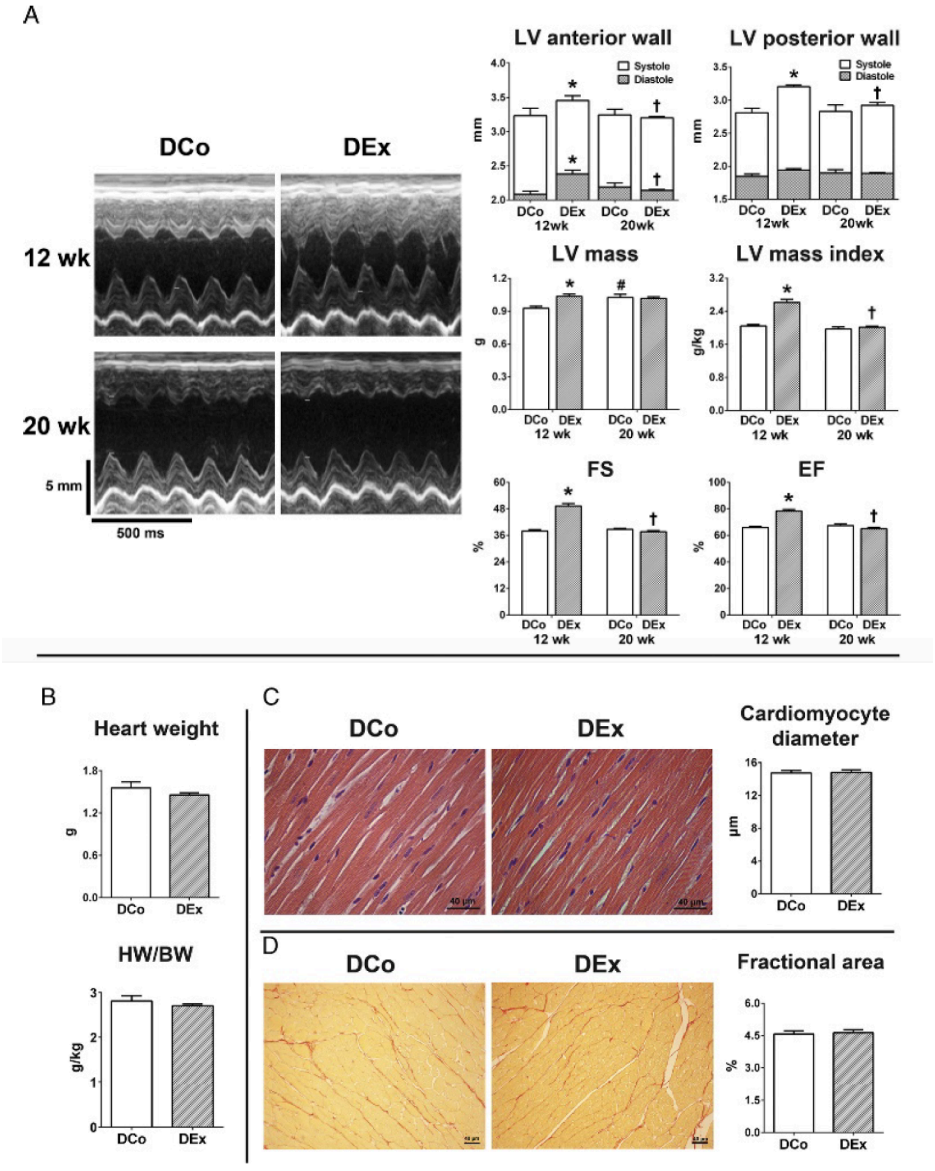

Figure 4. Markers of LV hypertrophy. A, M-mode echocardiography recordings of the LV from representative DCo and DEx rats at weeks 12 and 20 from. LV anterior and posterior wall thickness, LV mass and LV mass index values increased significantly after training (12 wk). Traditional LV systolic parameters (FS and EF) improved significantly after the completion of the training protocol. These parameters regressed completely after

8 weeks of detraining. **B,** Postmortem measured heart weight and heart weight to-body weight (HW/BW) ratios were equal in the detrained rats. **C,** Representative images of the LV myocardium after H&E staining. Cardiomyocyte diameters showed no difference between DEx and DCo groups. Magnification 400x; scale bar, 40 µm. **D,** Picrosirius red staining showed physiological LV collagen content (red staining) in both groups. Collagen fractional area did not differ in DEx and DCo rats. Magnification 200x; scale bar, 40 µm. n=8/group, *p< 0.05 DEx vs DCo at week 12; #p < 0.05 DCo at week 20 vs DCo at week 12; †p < 0.05 DEx at week 20 vs DEx at week 12.

This is a non-final version of an article published in final form in Oláh A, Kellermayer D, Mátyás C, Németh BT, Lux Á, Szabó L, Török M, Ruppert M, Meltzer A, Sayour AA, Benke K, Hartyánszky I, Merkely B, Radovits T. Complete Reversion of Cardiac Functional Adaptation Induced by Exercise Training. Med Sci Sports Exerc. 2017 Mar;49(3):420-429 (168).

(https://journals.lww.com/acsm-msse/Fulltext/2017/03000/Complete_Reversion_of_Cardiac_Functional.5.aspx)

3.2. Alterations in titin content and phosphorylation in athlete's heart

3.2.1. Titin isoform analysis in exercise-induced LV hypertrophy

We measured titin isoform ratios to assess the effect of long-term exercise on titin content (Figure 5A-B). N2BA/N2B increased significantly in the Ex group (Figure 5C), indicating a shift towards the more compliant titin isoform. The relative expression of total titin (TT) to myosin hevay chain (MHC) (Figure 5D) and the proteolytic degradation product T2 to TT (Figure 5E) showed no differences in the Co and Ex groups.

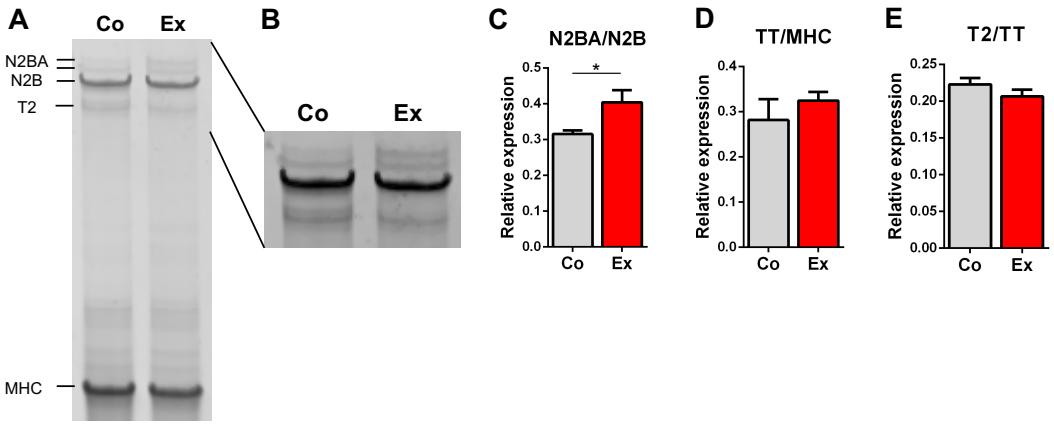

Figure 5. Titin isoform analysis. A, Example gel electrophoresis image of a Co and Ex LV sample. **B,** Linear contrast adjustment has also been applied to the original image for better visualization. **C,** The N2BA/N2B ratio increased significantly in exercised rats, indicating increased expression of the more compliant isoform. **D,** Total titin (TT) to Myosin Heavy Chain (MHC) ratio and **E,** the titin degradation product T2 over TT did not differ between the two groups. n=6/group, *p<0.05

3.2.2. Titin site-specific phosphorylation is modified after long-term exercise

We investigated total titin phosphorylation and site-specific phosphorylation in titin's PEVK region (PS11878, PS12022). Total titin phosphorylation did not differ between the two groups (Figure 6A). However, we detected hypophosphorylation of the PS11878 site (Figure 6B) and unaltered PS12022 phosphorylation (Figure 6C), indicating an exercise-specific phosphorylation effect.

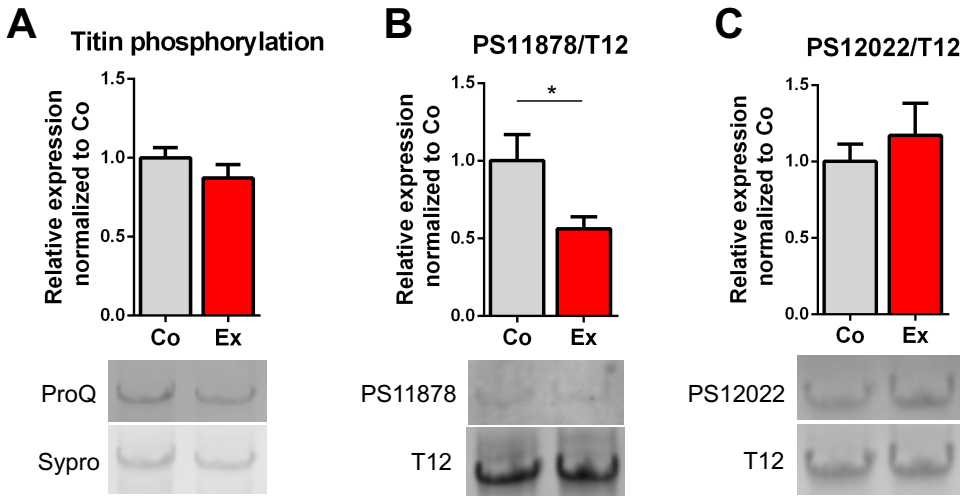

Figure 6. Long-term exercise alters titin's phosporylation. A, Total titin phosphorylation did not show any differences between control and exercised rats. **B,** Exercise resulted hypophosphorylation of titin's S11878 (S26) site (linear contrast adjustment was applied to the original PS11878 image for better visualization), **C,** but had no effect on the phosphorylation level of S12022 (S170). n=6/group, *p<0.05.

DOI:10.14753/SE.2022.2759

3.3. Sarcomere structure and elasticity of exercised cardiac myofibrils

Atomic force microscopy measurements revealed slight differences in the sarcomeric structural dimensions of single permeabilized exercised cardiac myofibrils compared to controls (Figure 7A) (n = 63 Co vs. n = 52 Ex sarcomeres). We observed well recognizable sarcomeric structure. However, we noticed greater flexibility and more curved structrue of the exercised myofibrils. Sarcomeric structure distances were measured on the contour profile of each myofibril. The sarcomere length (SL) was determined as the distance between the peaks of two neighboring Z-disks. The I-band length was measured as the length between the two deepest points surrounding the Z-disk. The distance between the two deepest points surrounding the M-band determined the A-band length (Figure 7B). We measured each sarcomere along 3 paraxial contour profiles to account for skew. Significantly shorter SL was measured in the Ex myofibrils (Co = 1.81 ± 0.01 µm vs. Ex = 1.73 ± 0.02 µm, p <0.01) (Figure 7C). Nevertheless, the SL was in the physiological slack length range (1.7–2.2 µm) in the Co and Ex groups. No alterations were seen in the I-band length/SL and the A-band length/SL in the two groups (Figure 7D). We did not find differences in the I-band/Z-disk height and the I-band/M-band height between the Co and Ex myofibrils (Figure 7E). The Z-disk/M-band height decreased significantly in the exercised myofibrils (Figure 7F). Overall, the Ex myofibrils displayed an irregular contour and surface profile while control myofibrils retained a more regular sarcomeric structure.

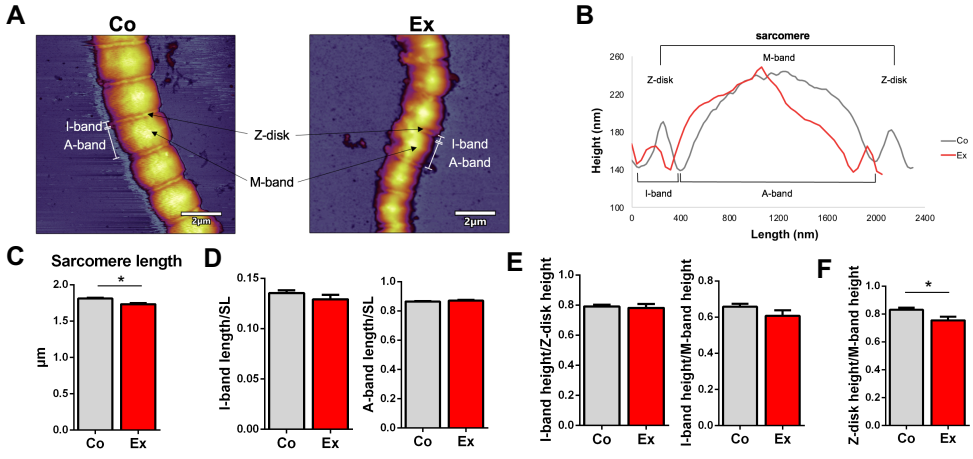

Figure 7. Sarcomeric and topographical structure of control and exercised myofibrils. A, Representative AFM images of a Co and Ex myofibril demonstrating the sarcomere structure. The Ex myofibril has more flexible and bended sarcomeres. **B,**

Representative topographical surface profile of a control and exercise sample. **C,** We found significantly shorter sarcomere lengths (SL) in the exercised group. **D,** No differences were revealed in the I-band length/SL and A-band length/SL between the two groups. **E,** The I-band height/Z-disk height and A-band height/Z-disk height was unaltered in the Co and Ex rats. **F,** The Z-disk height/M-band height was decreased in the Ex group. n=63 Co sarcomeres (4 hearts) vs. n=52 Ex sarcomeres (3 hearts) , *p<0.05.

In order to evaluate the lateral stiffness of Co and Ex sarcomeres, fast force mapping (FFM) was performed (Figure 8A). In FFM mode each pixel represents a force curve. We obtained the Young's modulus with the Johnson–Kendall–Roberts (JKR) fitting model of the force curves. The Young's modulus was significantly decreased in the Ex myofibrils (Co = 3.56 ± 1.17 MPa vs. Ex = 1.35 ± 1.51 MPa, $p < 0.01$), indicating improved sarcomeric compliance (Figure 8B). Conceivably, this causes the irregularity of the contour and surface profile of the exercised myofibrils.

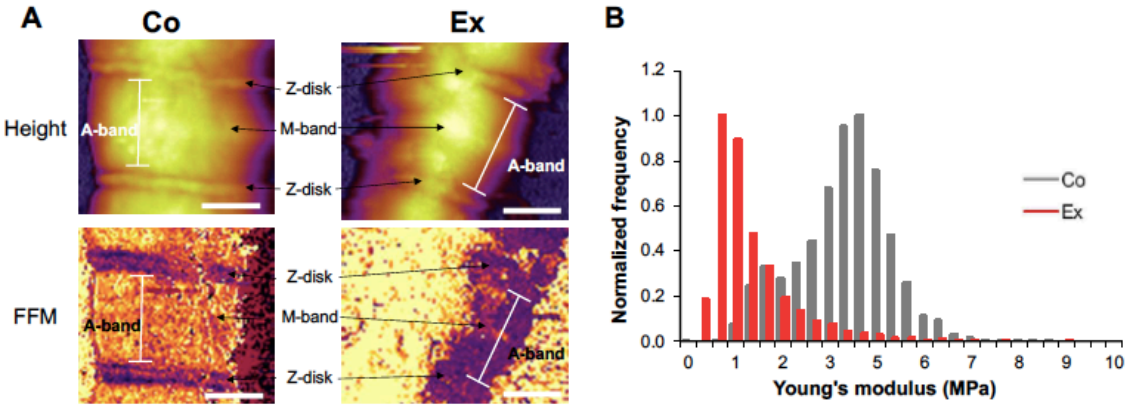

Figure 8. Fast force mapping of sarcomeres with AFM. A, Representative height image and stiffness map of a control and exercised sarcomere at a trigger force of 500 pN. **B,** The Young's modulus was significantly decreased in the Ex group vs. Co. Young's modulus was calculated by using the Johnson-Kendall-Roberts (JKR) fitting model. Note that the Ex sarcomere showed more perturbation. Scale bar 1µm.

3.4. Effects of detraining on cardiac morphology

The LV anterior and posterior wall thickness, LV mass and LV mass index of the DEx group showed complete regression after 8 weeks of detraining (Figure 4A). The EF and

FS also equalized in the control and exercised groups after deconditioning (Figure 4A). Furthermore, the heart weight and heart weight-to body weight ratio did not differ between the groups after the cessation of the training (Figure 4B). Even more, cardiomyocyte diameters were equal in the DCo and DEx rats (Figure 4C). LV collagen, determined with picrosirius red staining, was unaltered in the two groups after the detraining period (Figure 4D). Overall, these parameters reflect complete reversion of exercise-induced LV morphology to baseline level after 8 weeks of detraining.

3.5. Cardiac function after deconditioning

3.5.1. Baseline haemodynamic parameters

Left ventricular pressure-volume analysis revealed similar LV pressure and dP/dt data in the DCo and DEx groups (Figure 9.). The P-V loops completely overlap in the two groups, further indicating similar haemodynamic conditions of the DEx and DCo rats. Consequently, no differences were found in the baseline haemodynamic parameters (HR, MAP, LVESP, LVEDP, LVEDV, LVESV, SV, TPR) in the DEx and DCo animals after the detraining period (Table 2).

Table 2. Haemodynamic parameters of DCo and DEx rats

Values are mean ± SEM. HR: heart rate; MAP: mean arterial pressure; LVESP: left ventricular end-systolic pressure; LVEDP: left ventricular end-diastolic pressure; LVEDV: left ventricular end-diastolic volume; LVESV: left ventricular end-systolic volume; SV: stroke volume; CO: cardiac output, CI: cardiac index; EF: ejection fraction; TPR: total peripheral resistance; dP/dt_{max} and dP/dt_{min}: maximal slope of the systolic pressure increment and the diastolic pressure decrement, respectively; τ: time constant of LV pressure decay; ESPVR: end-systolic pressure-volume relationship; EDPVR: end-diastolic pressure-volume relationship; PRSW: prelaod recruitable stroke work; dP/dt_{max}-EDV: slope of dP/dt_{max} -end-diastolic volume relationship; SW: stroke work; Eff: mechanical efficiency, Ea: arterial elastance; VAC: ventriculo-arterial coupling.

This is a non-final version of an article published in final form in Oláh et al. (168).

	DCo (n=8)	DEx (n=8)	p
HR (BPM)	247 ± 8	249 ± 11	0.888
MAP (mmHg)	82.4 ± 2.5	795. ± 2.4	0.419
LVESP (mmHg)	102.7 ± 2.5	101.0 ± 4.2	0.723
LVEDP (mmHg)	6.6 ± 0.9	7.6 ± 1.0	0.452
LVEDV (µl)	253.0 ± 12.7	250.4 ± 13.2	0.890
LVESV (µl)	109.1 ± 4.4	105.7 ± 5.8	0.642
SV (µl)	143.9 ± 9.6	144.8 ± 9.0	0.949
CO (mL/min)	35.6 ± 2.6	35.9 ± 2.2	0.916
CI ((ml/min)/100g)	6.4 ± 0.4	6.7 ± 0.4	0.573
EF (%)	56.6 ± 1.4	57.7 ± 1.3	0.563
TPR (mmHg/(ml/min)	2.37 ± 0.12	2.25 ± 0.09	0.400
dP/dt_{max} (mmHg/s)	7084 ± 255	6903 ± 340	0.677
dP/dt_{min} (mmHg/s)	-7528 ±216	-7323 ± 262	0.564
τ, Glantz (ms)	11.3 ± 0.4	11.5 ± 0.3	0.760
ESPVR (mmHg/µl)	1.66 ± 0.12	1.60 ± 0.06	0.655
EDPVR (mmHg/µl)	0.029 ± 0.004	0.029 ± 0.004	0.914
PRSW (mmHg)	70.9 ± 2.4	69.5 ± 2.7	0.709
dP/dt_{max} – EDV ((mmHg/s)/µl)	34.0 ± 1.9	34.2 ± 1.8	0.949
SW (mmHg/ml)	12.6 ± 0.9	12.3 ± 0.6	0.831
PVA (mmHg/ml)	19.5 ± 1.9	19.8 ± 1.1	0.856
Eff (%)	69.4 ± 1.8	68.7 ± 1.2	0.742
E_a (mmHg/µl)	0.70 ± 0.03	0.71 ± 0.09	0.796
VAC	0.45 ± 0.04	0.45 ± 0.03	0.907

DOI:10.14753/SE.2022.2759

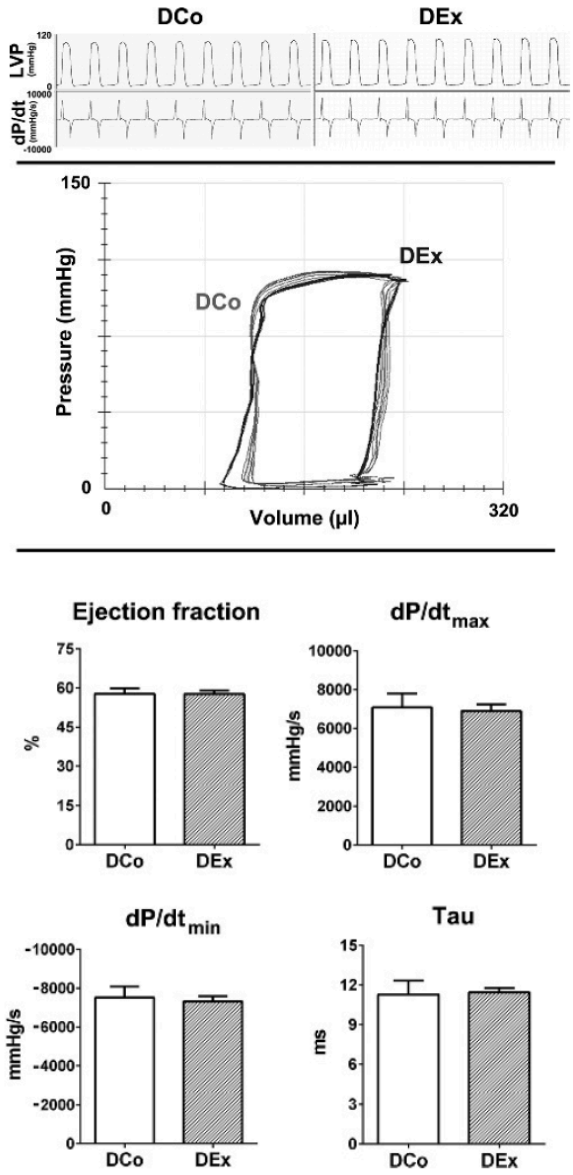

Figure 9. Steady-state P–V relations. *Upper panel*: recordings of LV pressure (LVP) and dP/dt signals from one representative DCo and DEx rat. *Mid panel:* representative steady-state P–V loops obtained from one DCo and DEx rat. The P–V loops of the two groups almost overlap each other, indicating similar pressure and volume values after detraining. *Lower panel:* no differences were revealed in the classic parameters of systolic (EF; dP/dt_{max}, maximal slope of the systolic pressure increment) and diastolic (dP/dt_{min}, maximal slope of the diastolic pressure decrement; Tau (τ): time constant of LV pressure decay) function. This is a non-final version of an article published in final form in Oláh et al. (168).

DOI:10.14753/SE.2022.2759

3.5.2. Cardiac contractility

The systolic parameters obtained via P-V analysis did not differ in the DEx rats compared to the DCo group after deconditioning. EF, CO, CI, dP/dt_{max} showed complete regression after the 8-week-long detraining period (Table 2, Figure 9.). We also acquired load-independent specific contractility indices by the occlusion of the inferior vena cava during P-V recordings (Figure 10.). The ESPVR, PRSW and dP/dt_{max} -EDV parameters were equal after detraining.

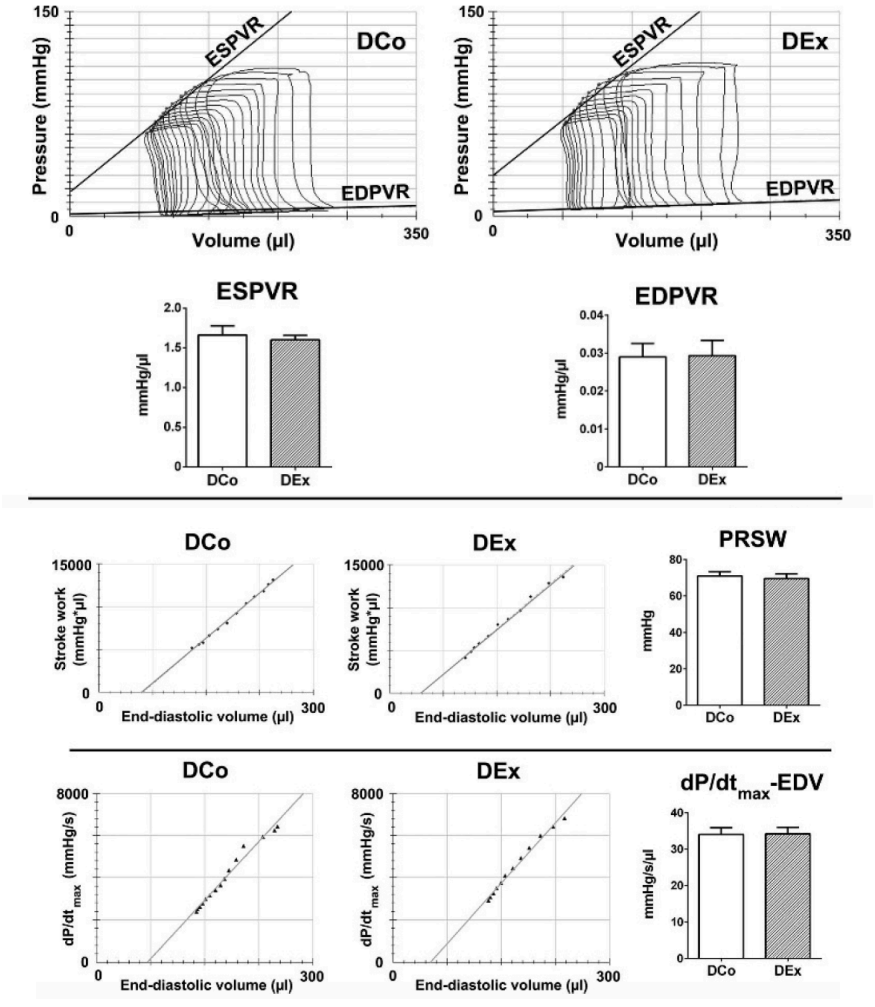

Figure 10. Load-independent parameters derived from left ventricular P–V analysis at different preloads during transient occlusion of the vena cava inferior. *Upper panel:* LV P–V loops recorded at different preloads. Slope of ESPVR (index of LV contractility) and slope of EDPVR (index of LV stiffness) in one representative animal

from DCo and DEx groups. These parameters were unaltered in the DEx rats compared to that of DCo animals after 8 weeks of detraining. *Mid and lower panel:* PRSW (the slope of the relationship between SW and end-diastolic volume) and maximal slope of the systolic pressure increment (dP/dt_{max})–end-diastolic volume relationship (dP/dt_{max}-EDV) from one representative rat from the DCo and DEx groups, respectively. These load-independent contractility indices showed no differences after the detraining period, reflecting similar inotropic state in detrained animals. This is a non-final version of an article published in final form in Oláh et al. (168).

3.5.3. Diastolic parameters

We evaluated the diastolic function of the heart after detraining. The active relaxation parameters, dP/dt_{min} and τ were unaltered in the DCo and DEx animals (Table 2, Figure 9). LVEDP and EDPVR, that describe the passive stiffness of the heart, also showed no differences in the DEx group compared to DCo rats (Table 2, Figure 10.).

3.5.4. Mechanoenergetic status of the heart

The mechanoenergetic condition of the heart was comparable in the detrained rats (Figure 11.). No differences were found in the stroke work (SW), pressure-volume area (PVA) and mechanical efficiency in the two groups. Furthermore, the ventriculo-arterial coupling (VAC), determined by arterial elastance and and ESPVR was equal in the DCo and DEx animals. All together, the functional (systolic, diastolic) performance and mechanoenergetic status of the athlete's heart is completely reversible after the cessation of training.

DOI:10.14753/SE.2022.2759

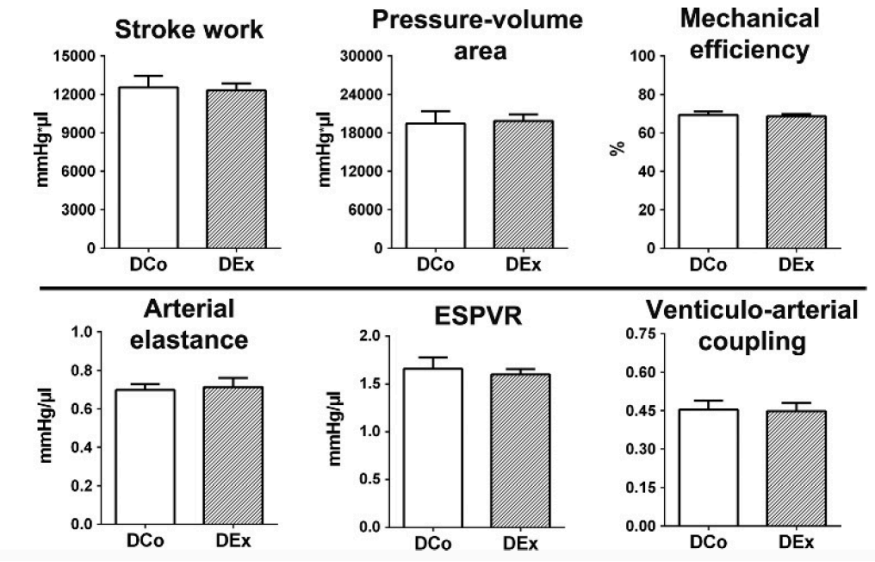

Figure 11. Cardiac mechanoenergetics. Similar values of LV SW and PVA in the detrained groups led to unaltered mechanical efficiency between the two groups after deconditioning. Unaltered E_a and LV contractility (ESPVR) resulted in similar ventriculo-arterial coupling (VAC) in the DEx and DCo rats. This is a non-final version of an article published in final form in Oláh et al (168).

4. Discussion

The heart adapts to regular physical activity resulting in morphological and functional cardiovascular changes, termed athlete's heart (2-4, 6, 7). In the past decades, the athletes's heart phenomenon has become the focus of interest in sports cardiology as there are increasing numbers of top-level athletes (155, 169). Moreover, there is a demand for improved physical fittness in the general population as well (17, 155, 170). Athlete's heart is a benign, physiological and reversible condition (6, 7, 11, 19). It has been well documented that regular aerobic exercise induces hypertrophy of the cardiac chambers, i.e. atria and the ventricles (7, 15, 16, 171-173). Moreover, it is accompanied by improved contractility, relaxation and mechanoenergetic status (7, 9, 12, 28, 174). It has been recognized that athlete's heart is also associated with supernormal left ventricular compliance (2, 48, 49). Cardiac compliance is mainly regulated by the giant elastic protein titin (49, 91). However, titin alterations induced by long-term endurance exercise and its potential contribution to the improved functional performance of athlete's heart have not been studied completely.

Additionally, previous human and animal studies have revealed that exercise-induced cardiac morphological alterations are completely reversible after detraining (7, 10, 13, 62, 143, 150). However, the specific deconditioning period required for structural regression has not been defined yet. Furthermore, the functional consequences of the cessation of training are still unclear. Thus, additional comprehensive research is required to reveal the reversibility of the functional parameters of athlete's heart. Importantly, in some cases, exercise-induced cardiac hypertrophy falls into the 'grey zone' and displays similar features of pathological conditions (7, 10, 22). Therefore, it is crucial to distinguish athlete's heart from pathological diseases and short-term deconditioning could contribute to the differential diagnostics (9, 11, 152, 155).

In the present study we provide further assessment of the cardiac adaptation to exercise on the cellular and molecular level. We characterize titin content and post-translational phosphorylation alterations in the rat model of exercise-induced left ventricular hypertrophy and its impact on myofibril structure and elasticity. Furthermore, we evaluate the functional reversibility of athlete's heart after an 8-week-long detraining period by using *in vivo* pressure-volume analysis.

4.1. Induction of athlete's heart by 12-week-long swimming training

Several exercise protocols have been established to induce cardiac hypertrophy, hence athlete's heart, to investigate the effects of physical activity on the cardiovascular system (29, 159, 160). According to our previously published protocol, we used a 12-week-long swimming training to induce athlete's heart in a rat model (12). Swimming exercise is a well regulated, balanced endurance training (12, 159, 165). In the current study, the exercised rats swam 120 min/day 5 days/week. In order to eliminate the effects of stress caused by water, control animals also swam 5 min/day 5 days/week. Our research group has previously evaluated the morphological and functional properties of the athlete's heart in detail (12, 28, 44). In accordance with our previous data, in the current study, we found significantly increased left ventricular wall dimensions (anterior and posterior wall thickness), LV mass and LV mass index in the exercised group. The EF and FS also improved significantly in the trained rats. Moreover, HW/BW, HW/TL ratios increased significantly after the 12-week-long training period. Therefore, athlete's heart has developed after the swimming protocol.

4.2. Alterations in titin isoform expression induced by long-term exercise

The main regulator of passive stiffness in cardiac and skeletal muscle is the giant elastic protein, titin (49, 91). It has been previously discussed, that titin-based passive stiffness also predicts exercise tolerance (49). Due to alternative splicing by RBM20, titin has two main isoforms in the adult cardiac muscle; the longer, and more compliant N2BA titin and the shorter and stiffer N2B titin (96, 106). Overall passive stiffness in cardiac muscle is defined by the ratio of these isoforms (98, 99, 110). Importantly, elevated N2BA expression, hence increased N2BA/N2B titin ratio is associated with reduced passive stiffness (98, 99, 103, 110). Furthermore, reduced titin-based passive stiffness corresponds to improved cardiac compliance (49). A hallmark study by Nagueh et al. also reported ameliorated exercise tolerance in patients with dilated cardiomyopathy who had increased N2BA/N2B ratio (110).

In our study we showed significantly increased N2BA/N2B titin ratio in exercised animals, suggesting a more compliant heart after swimming training compared to controls. We did not detect any differences in total titin content or T2 expression in the two groups. The study of Hidalgo et al., in accordance with Slater et al. did not reveal

titin isoform alterations after 3-6 weeks voluntary wheel running in mice (63, 117). However, recently Chung et al. published an elevated titin isoform ratio in exercised rats (131). It is important to note, that in their study rats performed exercise training on voluntary running wheels for 12 weeks (131). Even though voluntary wheel running is an accepted training method for exercise-induced cardiac hypertrophy (159), our swimming training is more rigorous, regulated and minimizes the different biological responses to exercise (12). Furthermore, it mimics the training program of top-level athletes (12). Nevertheless, our findings on titin isoform modifications induced by exercise is in accordance with the study of Chung et al.

Overall, we propose that long-term regular physical activity induces a shift towards the more compliant titin isform resulting in the upregulation of the N2BA/N2B ratio. Moreover, the elevated N2BA titin is a possible adaptive mechanism to the increased diastolic demand of the heart, induced by exercise.

4.3. Titin's post-translational phosphorylation modifications in the athlete's heart

Phosphorylation is the most extensively investigated post-translational modification process of titin (115). Although titin has several phosphorylation sites, a few well-recognized motifs have been evaluated in the N2B unique sequence and the PEVK region (63, 116-119, 122, 125). We found no alterations in total titin phosphorylation, that is in line with the findings of Chung et al (131). However, by the evaluation of specific phosphosites, we showed significant hypophosphorylation of the Ser11878 site, while the phosphorylation of the Ser12022 residue remained unaltered. This points to reduced titin-based passive stiffness of the heart after long-term exercise. Our results are in agreement with the study of Slater et al. that reported reduced phosphorylation of the Ser11878 residue after 3 weeks of voluntary wheel running (63). They additionally showed hyperphosphorylation of the Ser4010 site in the N2B-us (63). However, Hidalgo et al. demonstrated hypophosphorylation of the Ser12022 residue, while the phosphorylation of Ser11878 remained unchanged (117). The PKCα possibly has a higher affinity to Ser11878 that may indicate the distinct phosphorylation patterns (175). Overall, chronic exercise reduces titin-based passive stiffness (63, 117). On the contrary, it has been revealed that Ser4099 is hypophosphorylated in the N2B-us, while Ser11878 is

hyperphosphorylated in the PEVK element in rat LV samples after a single bout of 15 min treadmill running (125). This leads to increased titin-based passive stiffness and may contribute to the Frank-Starling mechanism, thereby resulting a quicker adaptation to the rapid volume changes in the heart (53, 125).

In summary, our findings suggest that passive stiffness is reduced in the athlete's heart via the hypophosphorylation of titin's PEVK element.

4.4. Evaluation of the structure and elasticity of cardiac myofibrils after chronic exercise

In order to evaluate whether long-term exercise affects sarcomeric stiffness, we analyzed the transverese elasticity of single myofibrils after chronic exercise. Myofibrils were isolated from the LV of rats after 12-week-long swimming training (176, 177). Atomic force microscopy was used to image and mechanically manipulate single myofibrils under buffer solution at room temperature (178). Myofibrils were subsrate-attached to a mica surface, generally used in AFM (137, 179). To enhance the fixation to the surface, we introduced an additional rapid centrifuge step, that affected the Ex myofibrils to a higher degree compared to control samples. We recognized the sarcomere structure in both groups by resonant (non-contact/AC-mode) scanning (178). However, exercised myofibrils displayed more flexible sarcomeres and greater level of irregularities, while control myofibrils showed straighter sarcomeres. This could be explained by the mechanical effects of exercise. Although sarcomere lengths (SL) were in the in vivo working length in both groups (1.7-2.2 μm) (95), we recognized slightly shorter SL in the exercised myofibrils. The I-band region of titin functions as a molecular spring (91, 180) and we propose that a larger relative amount of the more compliant N2BA isoform may allow larger amplitude contractions. This could potentially explain the more irregular and shorter sarcomeres of the exercised myofibrils. Furthermore, although 2,3-butanedione-monoxime (BDM) was added in the myofibril permeabilization solution to prevent further contractions of the samples (177), it is possible that internal stores of ATP could have contributed to additional sarcomere shortening (181).

We determined the length of the different sarcomeric structures based on the study of Ogneva et al (182). We did not see any alterations in the I-band/SL and A-band/SL in

the two groups. Moreover, the Co and Ex myofibrils did not show any differences in the I-band height/Z-diks height and I-band height/M-band height. However, the Z-disk height-to M-band height was significantly decreased in the exercised myofibrils. It is plausible that the exercised myofibrils became more flattened due to the centrifuge step. We also investigated the Young's modulus (elastic modulus) of the myofibrils exposed to chronic exercise, by fast force mapping (FFM) mode of the AFM (138, 139, 182). The Young's modulus of the Ex myofibrils was significantly decreased, indicating reduced passive-stiffness. Even though we revealed differences in titin isoform and site-specific phosphorylation localized in the I-band, the mechanical alterations were manifested across the entire sarcomere. Further molecular evaluation is required to explain this phenomenon. To date, only few groups analyzed the Young's modulus of striated muscle by FFM. A study by Li et al. reported that titin contributes to A-band lateral stiffness in psoas and diaphragm muscles and thus may be involved in active contraction (140). Akiyama et al. demonstrated lower Young's modulus of control cardiac myofibrils compared to our results (183). However, it is important to emphasize that they evaluated neonatal LV muscle, containing the fetal titin that is known to be the most compliant titin isoform (99, 128, 129). Nevertheless, to our knowledge, this is the first study to examine the elasticity of adult cardiac control and exercised myofibrils by fast force mapping.

In summary, our results demonstrate that long-term exercise leads to increased sarcomeric compliance in cardiac muscle. We propose that the changes in sarcomeric mechanics are related to the modifications in the titin isoform ratio and the PEVK element phosphorylation. Moreover, we speculate that this is an additional mechanism to aid the physiological adaptation of the heart in response to chronic exercise. Nonetheless, we evaluated samples from male rats, thus further investigations would be needed to examine whether any gender differences are present in titin alterations induced by exercise.

4.5. Left ventricular morphology after detraining

Numerous research groups focused on the morphological reversibility of exercise-induced cardiac hypertrophy (10, 11, 148). Human studies revealed regression of structural parameters of athlete's heart after 2 months of deconditioning (10, 148). On the other hand, Bocalini et al. showed complete regression of chronic exercise-induced alterations after 2 weeks of detraining in a rodent model (62). However, it is important to

note, that in some cases the LV appears less responsive to deconditioning, suggesting that increased body-weight and recreational exercise may influence the morphological regression of athlete's heart (10, 151).

Our research group also demonstrated regression of exercise-induced LV morphology after the cessation of training by echocardiography (12, 26). Based on previous reports, there is a variability in the detraining time needed for regression (10, 14, 62, 184, 185). Therefore, we evaluated the effects of deconditioning on cardiac function after an 8-week-long detraining period to surely detect any structural and functional reversibility of the athlete's heart.

After the detraining period, we found no differences in the wall thickness parameters, LV mass and LV mass index by echocardiography in detrained control (DCo) and detrained exercised (DEx) rats. Even more, the basic functional parameters, EF and FS also returned to control levels after detraining. Furthermore, heart weight, heart weight-to-body weight ratio and the cardiomyocyte diameters also returned to baseline levels in the DEx group. These results indicate that the loss of hypertrophic stimuli signals via the cessation of training can revert the exercise-induced molecular and cellular adaptation to control parameters (185). Although it has been reported that chronic exercise may induce fibrotic remodeling in the myocardium (184, 186), our research group did not reveal increased collagen deposit or activation of pathological signaling markers in the athlete's heart (12). However, we wanted to evalute whether deconditionig has an effect on myocardial fibrosis. In the current study, we showed unaltered LV collagen content in both groups by picrosirius red staining after the 8-weeks-long detraining time. This is in agreement with the finding that the potentially arrhythmogenic collagen infiltrates are completely reversible (13). Additionally, the current consensus is that chronic exercise does not lead to myocardial fibrosis (187).

Overall, our data support the previous findings that exercise-induced LV hypertrophy is completely reversible after deconditioning. Furthermore, athlete's heart is not associated with fibrotic remodeling, even after the cessation of training.

4.6. Consequences of detraining on cardiac function

4.6.1. Baseline pressure-volume (P-V) parameters

Regular training improves the cardiovascular capacity in order to adapt to the increased circulatory demand of exercise (3, 7, 16). As a consequence of the increased vagal tone associated with exercise, athletes often present sinus bradycardia (64, 188). However, Evangelista et al. demonstrated the loss of resting bradycardia after 2 weeks of detraining (189). Accordingly, we showed equal heart rates (HR) in our groups by P-V measurements after 8 weeks of deconditioning. Moreover, we found no differences in the pressure parameters (MAP, LVESP, LVEDP) between DCo and DEx rats. Stroke volume (SV) is signficantly improved in athlete's heart that is associated with a slight degree of LV dilation, thereby increased EDV (13, 21, 190). However, we previously reported no diffenreces in LVEDV, along with reduced LVESV in our athlete's heart rat model (12). This leads to significantly increased stroke volume and EF in exercise-induced LV hypertrophy (12). After deconditioning, we showed that SV and EF regressed to control levels in the DEx group as demonstrated on the baseline P-V loops. Our results are in line with the study of Martin et al., who found significantly reduced SV in top-level athletes after the cessation of training (191).

All together the baseline functional characteristics of athlete's heart completely regressed after the 8-week-long detraining period.

4.6.2. Systolic function

Most studies evaluate the cardiac morphology and function by noninvasive modalitites (7, 11, 51, 155). We found no differences regarding the traditional LV systolic parameteres between the detrained groups. EF, CO, CI and dP/dt_{max} were equal in the DCo and DEx animals. However, these values are highly dependent on loading conditions and HR (6, 192). Therefore, they might not display the enhanced systolic function of athlete's heart properly. However, P-V analysis is an effective tool to characterize the contractile function of the heart *in vivo* (12, 52, 54). In athlete's heart the 3 load-independent sensitive chronotropic indices, ESPVR, PRSW and dP/dt_{max}-EDV are significantly improved compared to sedentary controls (12, 28). In our current study, we did not reveal any differences in these parameters between the groups after detrainig. *In vitro* experimental studies on isolated cardiomyocytes and papillary muscles revealed

regression of exercise-induced contractility enhancement after 2-4 weeks (62, 150). Nevertheless, to our knowledge, this is the first *in vivo* pressure-volume analysis to evaluate the effects of detraining on cardiac function.

Overall, our results show complete reversibility of the improved exercise-induced cardiac function after 8 weeks of deconditioning.

4.6.3. Diastolic function

LV diastolic function is determined by the early, energy-dependent active relaxation and the late, passive relaxation (193, 194). Previous findings showed that athlete's heart is associated with improved active relaxation and unaltered or even enhanced passive relaxation (2, 12, 28, 48). However, after detraining no alterations were revealed regarding the load-dependent (dP/dt_{min}) and the load-independent (tau) values of active relaxation in the DCo and DEx groups. Alterations in EDPVR, the load-independent parameter of total LV stiffness may reflect changes in the collagen content of the myocardium (12, 195). Exercise-induced LV hypertrophy develops without increased interstitial fibrosis (13, 187). Furthermore, titin-based passive stiffness is reduced in the myocardium after long-term exercise (63). In our study, EDPVR was unchanged after deconditioning in the DEx rats compared to the DCo group. This is in agreement with human echocardiographic studies, which demonstrate regression of the enhanced diastolic function after deconditioning (192, 196).

Overall, our results point to complete regression of the improved exercise-induced active relaxation, hence diastolic function, after the cessation of training.

4.6.4. Mechanoenergetic status of the heart

Exercise-induced LV hypertrophy is characterized by improved metabolism and energetics, including enhanced glucose and fatty acid oxidation (72, 174, 197). In accordance with these findings, the *in vivo* analysis revealed improved LV efficiency in the athlete's heart, determined by stroke work (SW), the total LV mechanical work and by pressure-volume area (PVA), the total mechanical energy of cardiac contraction (12, 28, 198). The improved cardiac energetic parameters regressed completely after the 8-week-long detraining period in the DEx group.

Moreover, there is improved coupling between the LV and the arterial system in athlete's heart, described by ventriculo-arterial coupling (VAC) (12, 198). In our experiments VAC was also reverted after deconditioning.

These data suggest that the improved mechanoenergetic status of the athlete's heart regresses completely after 8 weeks of deconditioning.

Overall, athlete's heart is completely reversible after 8 weeks of inactivity. Thus, deconditioning is a truly beneficial tool to differentiate pathological and physiological conditions. Nevertheless, further evaluations may be required to determine the exact time point where morphological and functional reversibility of athlete's heart begins in order to prepare the best training plan for top-level athletes, with a special focus on the allowed number of resting days.

5. Conclusions

We evaluated titin alterations in the cardiac muscle after long-term exercise that mimics the training of top level athletes. The significantly increased N2BA/N2B titin ratio along with the decreased phosphorylation of titin's PEVK element suggests reduced titin-based passive stiffness and a more compliant heart after chronic exercise. The increased N2BA content possibly led to more flexible exercised myofibrils. To our knowledge, this is the first study to reveal decreased Young's modulus in cardiac myofibrils of the athlete's heart that is associated with decreased passive stiffness and more compliant conditions. Overall, titin modifications in the athlete's heart are potential mechanisms to improve cardiac compliance and provide the best adaptation and performance to the increased circulatory demand of long-term exercise.

Additionally, we investigated the effects of detraining on the athlete's heart. We revealed complete morphological and functional regression of exercise-induced cardiac adaptation after 8 weeks of deconditioning. LV hypertrophy developed after the 12-week-long swimming training, that regressed completely after the cessation of training. The morphological reversibility of the physiological LV hypertrophy was not associated with altered LV collagen content. Based on our sensitive pressure-volume analysis, we demonstrated equal data of the contractility and relaxation parameters in the detrained control and exercised rats. Furthermore, the cardiac energetics did not show any differences in the detrained animals. All together, these results indicate morphological and functional reversibility of the exercise-induced LV hypertrophy and the improved myocardial contractility and mechanoenergetic status. Moreover, to the best of our knowledge, this is the first study to report functional reversibility of athlete's heart by *in vivo* P-V haemodynamic characterization.

6. Summary

Long-term exercise induces benign morphological and functional adaptation of the myocardium, referred to as athlete's heart. Exercise tolerance is associated with reduced myocardial passive stiffness. The main determinant of the passive stiffness of the heart muscle is titin. Titin-based passive stiffness may be modified by changes in titin isoform expression (altered N2BA/N2B) or via post-translational alterations, mainly phosphorylation. To date there is limited knowledge about titin's role in the cardiac adaptation after long-term exercise. Moreover, although the functional condition of athlete's heart in enchanced, the effects of detraining on left ventricular (LV) function is unclear.

Therefore, the purpose of this study was to evaluate the N2BA/N2B isoform ratio and titin's post-translational phosphorylation in the LV and to correlate the findings with the cardiac sarcomere structure and elasticity in a rat model of athlete's heart. In addition, our aim was to investigate the reversibility of the improved functional parameters of athlete's heart after detraining.

We induced athlete's heart by a 12-week-long swimming training. We showed significantly increased N2BA/N2B ratio (Ex 0.40±0.03 vs. Co 0.32±0.01) and hypopohosphorylation of titin's PEVK element at the Ser11878 residue (Ex 0.56±0.08 vs. Co 1±0.17) in the exercised group. Moreover, the sarcomeric elastic modulus was reduced in the exercised rats (Ex 1.35±1.51 MPa vs. Co 3.56±1.17 MPa). These data indicate decreased titin-based passive stiffness of the myocardium, that is potentially caused by a shift towards the expression of the more compliant titin isoform and softening of the PEVK element induced by post-translational phosphorylation. These alterations are manifested as local mechanical rearrangements within the cardiac sarcomere and may contribute to the improved cardiac compliance of athlete's heart.

After the training period, rats of the control and exercised group remained sedentary for 8 weeks. We revealed no differences in the LV wall thickness and cardiomyocyte diameter in the two groups after deconditioning. Furthermore, the improved contractility, relaxation and mechanoenergetic parameters of the athlete's heart were comparable to the control levels after the cessation of training. Our results demonstrate complete morphological regression of athlete's heart and reversibility of exercise-induced LV functional enhancement after 8 weeks of detraining.

7. References

1. Nystoriak MA, Bhatnagar A. (2018) Cardiovascular Effects and Benefits of Exercise. Front Cardiovasc Med, 5:135.
2. Zilinski JL, Contursi ME, Isaacs SK, Deluca JR, Lewis GD, Weiner RB, Hutter AM, Jr., d'Hemecourt PA, Troyanos C, Dyer KS, Baggish AL. (2015) Myocardial adaptations to recreational marathon training among middle-aged men. Circ Cardiovasc Imaging, 8:e002487.
3. D'Silva A, Sharma S. (2014) Exercise, the athlete's heart, and sudden cardiac death. Phys Sportsmed, 42:100-13.
4. Sharma S, Merghani A, Mont L. (2015) Exercise and the heart: the good, the bad, and the ugly. Eur Heart J, 36:1445-53.
5. Paffenbarger RS, Jr., Hyde RT, Wing AL, Hsieh CC. (1986) Physical activity, all-cause mortality, and longevity of college alumni. N Engl J Med, 314:605-13.
6. Prior DL, La Gerche A. (2012) The athlete's heart. Heart, 98:947-55.
7. Maron BJ, Pelliccia A. (2006) The heart of trained athletes: cardiac remodeling and the risks of sports, including sudden death. Circulation, 114:1633-44.
8. Fagard R. (2003) Athlete's heart. Heart, 89:1455-61.
9. Pelliccia A, Di Paolo FM, Maron BJ. (2002) The athlete's heart: remodeling, electrocardiogram and preparticipation screening. Cardiol Rev, 10:85-90.
10. Pelliccia A, Maron BJ, De Luca R, Di Paolo FM, Spataro A, Culasso F. (2002) Remodeling of left ventricular hypertrophy in elite athletes after long-term deconditioning. Circulation, 105:944-9.
11. Swoboda PP, Garg P, Levelt E, Broadbent DA, Zolfaghari-Nia A, Foley AJR, Fent GJ, Chew PG, Brown LA, Saunderson CE, Dall'Armellina E, Greenwood JP, Plein S. (2019) Regression of Left Ventricular Mass in Athletes Undergoing Complete Detraining Is Mediated by Decrease in Intracellular but Not Extracellular Compartments. Circ Cardiovasc Imaging, 12:e009417.
12. Radovits T, Olah A, Lux A, Nemeth BT, Hidi L, Birtalan E, Kellermayer D, Matyas C, Szabo G, Merkely B. (2013) Rat model of exercise-induced cardiac

hypertrophy: hemodynamic characterization using left ventricular pressure-volume analysis. Am J Physiol Heart Circ Physiol, 305:H124-34.

13. Benito B, Gay-Jordi G, Serrano-Mollar A, Guasch E, Shi Y, Tardif JC, Brugada J, Nattel S, Mont L. (2011) Cardiac arrhythmogenic remodeling in a rat model of long-term intensive exercise training. Circulation, 123:13-22.

14. Biffi A, Maron BJ, Verdile L, Fernando F, Spataro A, Marcello G, Ciardo R, Ammirati F, Colivicchi F, Pelliccia A. (2004) Impact of physical deconditioning on ventricular tachyarrhythmias in trained athletes. J Am Coll Cardiol, 44:1053-8.

15. Morganroth J, Maron BJ, Henry WL, Epstein SE. (1975) Comparative left ventricular dimensions in trained athletes. Ann Intern Med, 82:521-4.

16. Mihl C, Dassen WR, Kuipers H. (2008) Cardiac remodelling: concentric versus eccentric hypertrophy in strength and endurance athletes. Neth Heart J, 16:129-33.

17. Dores H, Freitas A, Malhotra A, Mendes M, Sharma S. (2015) The hearts of competitive athletes: An up-to-date overview of exercise-induced cardiac adaptations. Revista Portuguesa de Cardiologia (English Edition), 34:51-64.

18. Ekblom B, Hermansen L. (1968) Cardiac output in athletes. J Appl Physiol, 25:619-25.

19. Pluim BM, Zwinderman AH, van der Laarse A, van der Wall EE. (2000) The athlete's heart. A meta-analysis of cardiac structure and function. Circulation, 101:336-44.

20. Fisman EZ, Embon P, Pines A, Tenenbaum A, Drory Y, Shapira I, Motro M. (1997) Comparison of left ventricular function using isometric exercise Doppler echocardiography in competitive runners and weightlifters versus sedentary individuals. Am J Cardiol, 79:355-9.

21. Csecs I, Czimbalmos C, Toth A, Dohy Z, Suhai IF, Szabo L, Kovacs A, Lakatos B, Sydo N, Kheirkhahan M, Peritz D, Kiss O, Merkely B, Vago H. (2020) The impact of sex, age and training on biventricular cardiac adaptation in healthy adult

and adolescent athletes: Cardiac magnetic resonance imaging study. Eur J Prev Cardiol, 27:540-9.

22. Czimbalmos C, Csecs I, Toth A, Kiss O, Suhai FI, Sydo N, Dohy Z, Apor A, Merkely B, Vago H. (2019) The demanding grey zone: Sport indices by cardiac magnetic resonance imaging differentiate hypertrophic cardiomyopathy from athlete's heart. PLoS One, 14:e0211624.

23. Albaeni A, Davis JW, Ahmad M. (2021) Echocardiographic evaluation of the Athlete's heart. Echocardiography, 38:1002-16.

24. Bjerring AW, Landgraff HE, Leirstein S, Aaeng A, Ansari HZ, Saberniak J, Murbraech K, Bruun H, Stokke TM, Haugaa KH, Hallen J, Edvardsen T, Sarvari SI. (2018) Morphological changes and myocardial function assessed by traditional and novel echocardiographic methods in preadolescent athlete's heart. Eur J Prev Cardiol, 25:1000-7.

25. Abergel E, Chatellier G, Hagege AA, Oblak A, Linhart A, Ducardonnet A, Menard J. (2004) Serial left ventricular adaptations in world-class professional cyclists: implications for disease screening and follow-up. J Am Coll Cardiol, 44:144-9.

26. Olah A, Kovacs A, Lux A, Tokodi M, Braun S, Lakatos BK, Matyas C, Kellermayer D, Ruppert M, Sayour AA, Barta BA, Merkely B, Radovits T. (2019) Characterization of the dynamic changes in left ventricular morphology and function induced by exercise training and detraining. Int J Cardiol, 277:178-85.

27. Basavarajaiah S, Boraita A, Whyte G, Wilson M, Carby L, Shah A, Sharma S. (2008) Ethnic differences in left ventricular remodeling in highly-trained athletes relevance to differentiating physiologic left ventricular hypertrophy from hypertrophic cardiomyopathy. J Am Coll Cardiol, 51:2256-62.

28. Olah A, Matyas C, Kellermayer D, Ruppert M, Barta BA, Sayour AA, Torok M, Koncsos G, Giricz Z, Ferdinandy P, Merkely B, Radovits T. (2019) Sex Differences in Morphological and Functional Aspects of Exercise-Induced Cardiac Hypertrophy in a Rat Model. Front Physiol, 10:889.

29. Konhilas JP, Maass AH, Luckey SW, Stauffer BL, Olson EN, Leinwand LA. (2004) Sex modifies exercise and cardiac adaptation in mice. Am J Physiol Heart Circ Physiol, 287:H2768-76.

30. Foryst-Ludwig A, Kreissl MC, Sprang C, Thalke B, Bohm C, Benz V, Gurgen D, Dragun D, Schubert C, Mai K, Stawowy P, Spranger J, Regitz-Zagrosek V, Unger T, Kintscher U. (2011) Sex differences in physiological cardiac hypertrophy are associated with exercise-mediated changes in energy substrate availability. Am J Physiol Heart Circ Physiol, 301:H115-22.

31. Colombo C, Finocchiaro G. (2018) The Female Athlete's Heart: Facts and Fallacies. Curr Treat Options Cardiovasc Med, 20:101.

32. D'Andrea A, Riegler L, Golia E, Cocchia R, Scarafile R, Salerno G, Pezzullo E, Nunziata L, Citro R, Cuomo S, Caso P, Di Salvo G, Cittadini A, Russo MG, Calabro R, Bossone E. (2013) Range of right heart measurements in top-level athletes: the training impact. Int J Cardiol, 164:48-57.

33. Gati S, Sharma S. (2020) Determinants of the athlete's heart: a cardiovascular magnetic resonance imaging study. Eur J Prev Cardiol, 27:536-9.

34. Gati S, Sharma S, Pennell D. (2018) The Role of Cardiovascular Magnetic Resonance Imaging in the Assessment of Highly Trained Athletes. JACC Cardiovasc Imaging, 11:247-59.

35. Fogante M, Agliata G, Basile MC, Compagnucci P, Volpato G, Falanga U, Stronati G, Guerra F, Vignale D, Esposito A, Dello Russo A, Casella M, Giovagnoni A. (2021) Cardiac Imaging in Athlete's Heart: The Role of the Radiologist. Medicina (Kaunas), 57.

36. D'Andrea A, Cocchia R, Riegler L, Scarafile R, Salerno G, Gravino R, Golia E, Pezzullo E, Citro R, Limongelli G, Pacileo G, Cuomo S, Caso P, Russo MG, Bossone E, Calabro R. (2010) Left ventricular myocardial velocities and deformation indexes in top-level athletes. J Am Soc Echocardiogr, 23:1281-8.

37. Paterick TE, Gordon T, Spiegel D. (2014) Echocardiography: profiling of the athlete's heart. J Am Soc Echocardiogr, 27:940-8.

38. Boraita A, Sanchez-Testal MV, Diaz-Gonzalez L, Heras ME, Alcocer-Ayuga M, de la Rosa A, Rabadan M, Abdul-Jalbar B, Perez de Isla L, Santos-Lozano A, Lucia A. (2019) Apparent Ventricular Dysfunction in Elite Young Athletes: Another Form of Cardiac Adaptation of the Athlete's Heart. J Am Soc Echocardiogr, 32:987-96.

39. Perry R, Swan AL, Hecker T, De Pasquale CG, Selvanayagam JB, Joseph MX. (2019) The Spectrum of Change in the Elite Athlete's Heart. J Am Soc Echocardiogr, 32:978-86.

40. Scharf M, Brem MH, Wilhelm M, Schoepf UJ, Uder M, Lell MM. (2010) Atrial and ventricular functional and structural adaptations of the heart in elite triathletes assessed with cardiac MR imaging. Radiology, 257:71-9.

41. Bansal M, Kasliwal RR. (2013) How do I do it? Speckle-tracking echocardiography. Indian heart journal, 65:117-23.

42. D'Andrea A, Bossone E, Radmilovic J, Caso P, Calabrò R, Russo MG, Galderisi M. (2015) The role of new echocardiographic techniques in athlete's heart. F1000Research, 4:289.

43. Forsythe L, George K, Oxborough D. (2018) Speckle Tracking Echocardiography for the Assessment of the Athlete's Heart: Is It Ready for Daily Practice? Curr Treat Options Cardiovasc Med, 20:83.

44. Kovacs A, Olah A, Lux A, Matyas C, Nemeth BT, Kellermayer D, Ruppert M, Torok M, Szabo L, Meltzer A, Assabiny A, Birtalan E, Merkely B, Radovits T. (2015) Strain and strain rate by speckle-tracking echocardiography correlate with pressure-volume loop-derived contractility indices in a rat model of athlete's heart. Am J Physiol Heart Circ Physiol, 308:H743-8.

45. Tokodi M, Oláh A, Fábián A, Lakatos BK, Hizoh I, Ruppert M, Sayour AA, Barta BA, Kiss O, Sydó N, Csulak E, Ladányi Z, Merkely B, Kovács A, Radovits T. (2022) Novel insights into the athlete's heart: is myocardial work the new champion of systolic function? European heart journal Cardiovascular Imaging, 23:188-97.

46. Libonati JR. (1999) Myocardial diastolic function and exercise. Med Sci Sports Exerc, 31:1741-7.

47. Libonati JR, Colby AM, Caldwell TM, Kasparian R, Glassberg HL. (1999) Systolic and diastolic cardiac function time intervals and exercise capacity in women. Med Sci Sports Exerc, 31:258-63.

48. Apor A, Merkely B, Morrell T, Zhu S, Ghosh E, Vágó H, Andrássy P, Kovács SJ. (2013) Diastolic function in Olympic athletes versus controls: Stiffness-based and relaxation-based echocardiographic comparisons. Journal of Exercise Science & Fitness, 11:29-34.

49. Lalande S, Mueller PJ, Chung CS. (2017) The link between exercise and titin passive stiffness. Exp Physiol, 102:1055-66.

50. Notomi Y, Martin-Miklovic MG, Oryszak SJ, Shiota T, Deserranno D, Popovic ZB, Garcia MJ, Greenberg NL, Thomas JD. (2006) Enhanced ventricular untwisting during exercise: a mechanistic manifestation of elastic recoil described by Doppler tissue imaging. Circulation, 113:2524-33.

51. Lakatos BK, Molnar AA, Kiss O, Sydo N, Tokodi M, Solymossi B, Fabian A, Dohy Z, Vago H, Babity M, Bognar C, Kovacs A, Merkely B. (2020) Relationship between Cardiac Remodeling and Exercise Capacity in Elite Athletes: Incremental Value of Left Atrial Morphology and Function Assessed by Three-Dimensional Echocardiography. J Am Soc Echocardiogr, 33:101-9 e1.

52. Pacher P, Nagayama T, Mukhopadhyay P, Batkai S, Kass DA. (2008) Measurement of cardiac function using pressure-volume conductance catheter technique in mice and rats. Nat Protoc, 3:1422-34.

53. Methawasin M, Hutchinson KR, Lee EJ, Smith JE, 3rd, Saripalli C, Hidalgo CG, Ottenheijm CA, Granzier H. (2014) Experimentally increasing titin compliance in a novel mouse model attenuates the Frank-Starling mechanism but has a beneficial effect on diastole. Circulation, 129:1924-36.

54. Bastos MB, Burkhoff D, Maly J, Daemen J, den Uil CA, Ameloot K, Lenzen M, Mahfoud F, Zijlstra F, Schreuder JJ, Van Mieghem NM. (2020) Invasive left

ventricle pressure-volume analysis: overview and practical clinical implications. Eur Heart J, 41:1286-97.

55. Diffee GM. (2004) Adaptation of cardiac myocyte contractile properties to exercise training. Exerc Sport Sci Rev, 32:112-9.

56. Diffee GM, Nagle DF. (2003) Exercise training alters length dependence of contractile properties in rat myocardium. J Appl Physiol (1985), 94:1137-44.

57. Diffee GM, Seversen EA, Titus MM. (2001) Exercise training increases the Ca(2+) sensitivity of tension in rat cardiac myocytes. J Appl Physiol (1985), 91:309-15.

58. Kemi OJ, Haram PM, Loennechen JP, Osnes JB, Skomedal T, Wisloff U, Ellingsen O. (2005) Moderate vs. high exercise intensity: differential effects on aerobic fitness, cardiomyocyte contractility, and endothelial function. Cardiovasc Res, 67:161-72.

59. Bodi B, Olah A, Martha L, Toth A, Radovits T, Merkely B, Papp Z. (2021) Exercise-induced alterations of myocardial sarcomere dynamics are associated with hypophosphorylation of cardiac troponin I. Rev Cardiovasc Med, 22:1079-85.

60. Tibbits GF, Kashihara H, O'Reilly K. (1989) Na+-Ca2+ exchange in cardiac sarcolemma: modulation of Ca2+ affinity by exercise. Am J Physiol, 256:C638-43.

61. Pierce GN, Sekhon PS, Meng HP, Maddaford TG. (1989) Effects of chronic swimming training on cardiac sarcolemmal function and composition. J Appl Physiol (1985), 66:1715-21.

62. Bocalini DS, Carvalho EV, de Sousa AF, Levy RF, Tucci PJ. (2010) Exercise training-induced enhancement in myocardial mechanics is lost after 2 weeks of detraining in rats. Eur J Appl Physiol, 109:909-14.

63. Slater RE, Strom JG, Granzier H. (2017) Effect of exercise on passive myocardial stiffness in mice with diastolic dysfunction. J Mol Cell Cardiol, 108:24-33.

64. Sharma S, Drezner JA, Baggish A, Papadakis M, Wilson MG, Prutkin JM, La Gerche A, Ackerman MJ, Borjesson M, Salerno JC, Asif IM, Owens DS, Chung EH, Emery MS, Froelicher VF, Heidbuchel H, Adamuz C, Asplund CA, Cohen G, Harmon KG, Marek JC, Molossi S, Niebauer J, Pelto HF, Perez MV, Riding NR, Saarel T, Schmied CM, Shipon DM, Stein R, Vetter VL, Pelliccia A, Corrado D. (2018) International recommendations for electrocardiographic interpretation in athletes. Eur Heart J, 39:1466-80.

65. Drezner JA. (2012) Standardised criteria for ECG interpretation in athletes: a practical tool. Br J Sports Med, 46 Suppl 1:i6-8.

66. Sharma S, Papadakis M. (2015) Interpreting the Athlete's EKG: are all repolarization anomalies created equal? Circulation, 131:128-30.

67. Sharma S. (2018) Effects of International Electrocardiographic Interpretation Recommendations on African American Athletes. JAMA Cardiol, 3:75-6.

68. Maillet M, van Berlo JH, Molkentin JD. (2013) Molecular basis of physiological heart growth: fundamental concepts and new players. Nat Rev Mol Cell Biol, 14:38-48.

69. Bass-Stringer S, Tai CMK, McMullen JR. (2021) IGF1-PI3K-induced physiological cardiac hypertrophy: Implications for new heart failure therapies, biomarkers, and predicting cardiotoxicity. Journal of sport and health science, 10:637-47.

70. McMullen JR, Shioi T, Huang WY, Zhang L, Tarnavski O, Bisping E, Schinke M, Kong S, Sherwood MC, Brown J, Riggi L, Kang PM, Izumo S. (2004) The insulin-like growth factor 1 receptor induces physiological heart growth via the phosphoinositide 3-kinase(p110alpha) pathway. J Biol Chem, 279:4782-93.

71. McMullen JR, Shioi T, Zhang L, Tarnavski O, Sherwood MC, Kang PM, Izumo S. (2003) Phosphoinositide 3-kinase(p110alpha) plays a critical role for the induction of physiological, but not pathological, cardiac hypertrophy. Proc Natl Acad Sci U S A, 100:12355-60.

72. Moreira JBN, Wohlwend M, Wisloff U. (2020) Exercise and cardiac health: physiological and molecular insights. Nat Metab, 2:829-39.

73. Nakamura M, Sadoshima J. (2018) Mechanisms of physiological and pathological cardiac hypertrophy. Nat Rev Cardiol, 15:387-407.

74. McMullen JR, Amirahmadi F, Woodcock EA, Schinke-Braun M, Bouwman RD, Hewitt KA, Mollica JP, Zhang L, Zhang Y, Shioi T, Buerger A, Izumo S, Jay PY, Jennings GL. (2007) Protective effects of exercise and phosphoinositide 3-kinase(p110alpha) signaling in dilated and hypertrophic cardiomyopathy. Proc Natl Acad Sci U S A, 104:612-7.

75. Knoll R, Hoshijima M, Hoffman HM, Person V, Lorenzen-Schmidt I, Bang ML, Hayashi T, Shiga N, Yasukawa H, Schaper W, McKenna W, Yokoyama M, Schork NJ, Omens JH, McCulloch AD, Kimura A, Gregorio CC, Poller W, Schaper J, Schultheiss HP, Chien KR. (2002) The cardiac mechanical stretch sensor machinery involves a Z disc complex that is defective in a subset of human dilated cardiomyopathy. Cell, 111:943-55.

76. Granzier HL, Labeit S. (2004) The giant protein titin: a major player in myocardial mechanics, signaling, and disease. Circ Res, 94:284-95.

77. Shadrin IY, Khodabukus A, Bursac N. (2016) Striated muscle function, regeneration, and repair. Cell Mol Life Sci, 73:4175-202.

78. Clark KA, McElhinny AS, Beckerle MC, Gregorio CC. (2002) Striated muscle cytoarchitecture: an intricate web of form and function. Annu Rev Cell Dev Biol, 18:637-706.

79. Marcucci L, Bondi M, Randazzo G, Reggiani C, Natali AN, Pavan PG. (2019) Fibre and extracellular matrix contributions to passive forces in human skeletal muscles: An experimental based constitutive law for numerical modelling of the passive element in the classical Hill-type three element model. PLoS One, 14:e0224232.

80. Sanger JW, Ayoob JC, Chowrashi P, Zurawski D, Sanger JM. (2000) Assembly of myofibrils in cardiac muscle cells. Adv Exp Med Biol, 481:89-102; discussion 3-5.

81. Hanson J, Huxley HE. (1953) Structural basis of the cross-striations in muscle. Nature, 172:530-2.

82. Huxley HE. (1953) Electron microscope studies of the organisation of the filaments in striated muscle. Biochim Biophys Acta, 12:387-94.

83. Rassier DE. (2017) Sarcomere mechanics in striated muscles: from molecules to sarcomeres to cells. Am J Physiol Cell Physiol, 313:C134-C45.

84. Furst DO, Osborn M, Nave R, Weber K. (1988) The organization of titin filaments in the half-sarcomere revealed by monoclonal antibodies in immunoelectron microscopy: a map of ten nonrepetitive epitopes starting at the Z line extends close to the M line. J Cell Biol, 106:1563-72.

85. Labeit S, Kolmerer B. (1995) Titins: giant proteins in charge of muscle ultrastructure and elasticity. Science, 270:293-6.

86. Tskhovrebova L, Trinick J. (2003) Titin: properties and family relationships. Nat Rev Mol Cell Biol, 4:679-89.

87. Granzier HL, Labeit S. (2005) Titin and its associated proteins: the third myofilament system of the sarcomere. Adv Protein Chem, 71:89-119.

88. Huxley AF. (1957) Muscle structure and theories of contraction. Prog Biophys Biophys Chem, 7:255-318.

89. Powers JD, Malingen SA, Regnier M, Daniel TL. (2021) The Sliding Filament Theory Since Andrew Huxley: Multiscale and Multidisciplinary Muscle Research. Annu Rev Biophys, 50:373-400.

90. Allen DG, Kentish JC. (1985) The cellular basis of the length-tension relation in cardiac muscle. J Mol Cell Cardiol, 17:821-40.

91. Granzier HL, Irving TC. (1995) Passive tension in cardiac muscle: contribution of collagen, titin, microtubules, and intermediate filaments. Biophys J, 68:1027-44.

92. Granzier H, Kellermayer M, Helmes M, Trombitas K. (1997) Titin elasticity and mechanism of passive force development in rat cardiac myocytes probed by thin-filament extraction. Biophys J, 73:2043-53.

93. Martonosi AN. (2000) Animal electricity, Ca2+ and muscle contraction. A brief history of muscle research. Acta Biochim Pol, 47:493-516.

94. Rall JA. (2018) What makes skeletal muscle striated? Discoveries in the endosarcomeric and exosarcomeric cytoskeleton. Adv Physiol Educ, 42:672-84.

95. Weiwad WK, Linke WA, Wussling MH. (2000) Sarcomere length-tension relationship of rat cardiac myocytes at lengths greater than optimum. J Mol Cell Cardiol, 32:247-59.

96. Bang ML, Centner T, Fornoff F, Geach AJ, Gotthardt M, McNabb M, Witt CC, Labeit D, Gregorio CC, Granzier H, Labeit S. (2001) The complete gene sequence of titin, expression of an unusual approximately 700-kDa titin isoform, and its interaction with obscurin identify a novel Z-line to I-band linking system. Circ Res, 89:1065-72.

97. Tskhovrebova L, Trinick J. (2004) Properties of titin immunoglobulin and fibronectin-3 domains. J Biol Chem, 279:46351-4.

98. Granzier H, Labeit S. (2002) Cardiac titin: an adjustable multi-functional spring. J Physiol, 541:335-42.

99. Lahmers S, Wu Y, Call DR, Labeit S, Granzier H. (2004) Developmental control of titin isoform expression and passive stiffness in fetal and neonatal myocardium. Circ Res, 94:505-13.

100. Ait-Mou Y, Hsu K, Farman GP, Kumar M, Greaser ML, Irving TC, de Tombe PP. (2016) Titin strain contributes to the Frank-Starling law of the heart by structural rearrangements of both thin- and thick-filament proteins. Proc Natl Acad Sci U S A, 113:2306-11.

101. Freundt JK, Linke WA. (2019) Titin as a force-generating muscle protein under regulatory control. J Appl Physiol (1985), 126:1474-82.

102. Kruger M, Kotter S. (2016) Titin, a Central Mediator for Hypertrophic Signaling, Exercise-Induced Mechanosignaling and Skeletal Muscle Remodeling. Front Physiol, 7:76.

103. Linke WA. (2018) Titin Gene and Protein Functions in Passive and Active Muscle. Annu Rev Physiol, 80:389-411.

104. Tonino P, Kiss B, Strom J, Methawasin M, Smith JE, 3rd, Kolb J, Labeit S, Granzier H. (2017) The giant protein titin regulates the length of the striated muscle thick filament. Nat Commun, 8:1041.

105. Gotthardt M, Hammer RE, Hubner N, Monti J, Witt CC, McNabb M, Richardson JA, Granzier H, Labeit S, Herz J. (2003) Conditional expression of mutant M-line titins results in cardiomyopathy with altered sarcomere structure. J Biol Chem, 278:6059-65.

106. Guo W, Schafer S, Greaser ML, Radke MH, Liss M, Govindarajan T, Maatz H, Schulz H, Li S, Parrish AM, Dauksaite V, Vakeel P, Klaassen S, Gerull B, Thierfelder L, Regitz-Zagrosek V, Hacker TA, Saupe KW, Dec GW, Ellinor PT, MacRae CA, Spallek B, Fischer R, Perrot A, Ozcelik C, Saar K, Hubner N, Gotthardt M. (2012) RBM20, a gene for hereditary cardiomyopathy, regulates titin splicing. Nat Med, 18:766-73.

107. Neagoe C, Kulke M, del Monte F, Gwathmey JK, de Tombe PP, Hajjar RJ, Linke WA. (2002) Titin isoform switch in ischemic human heart disease. Circulation, 106:1333-41.

108. Cazorla O, Freiburg A, Helmes M, Centner T, McNabb M, Wu Y, Trombitas K, Labeit S, Granzier H. (2000) Differential expression of cardiac titin isoforms and modulation of cellular stiffness. Circ Res, 86:59-67.

109. Makarenko I, Opitz CA, Leake MC, Neagoe C, Kulke M, Gwathmey JK, del Monte F, Hajjar RJ, Linke WA. (2004) Passive stiffness changes caused by upregulation of compliant titin isoforms in human dilated cardiomyopathy hearts. Circ Res, 95:708-16.

110. Nagueh SF, Shah G, Wu Y, Torre-Amione G, King NM, Lahmers S, Witt CC, Becker K, Labeit S, Granzier HL. (2004) Altered titin expression, myocardial stiffness, and left ventricular function in patients with dilated cardiomyopathy. Circulation, 110:155-62.

111. Kellermayer D, Smith JE, 3rd, Granzier H. (2017) Novex-3, the tiny titin of muscle. Biophys Rev, 9:201-6.

112. Zou J, Tran D, Baalbaki M, Tang LF, Poon A, Pelonero A, Titus EW, Yuan C, Shi C, Patchava S, Halper E, Garg J, Movsesyan I, Yin C, Wu R, Wilsbacher LD, Liu J, Hager RL, Coughlin SR, Jinek M, Pullinger CR, Kane JP, Hart DO, Kwok PY, Deo RC. (2015) An internal promoter underlies the difference in disease severity between N- and C-terminal truncation mutations of Titin in zebrafish. Elife, 4:e09406.

113. Huang J, Zhu X. (2016) The molecular mechanisms of calpains action on skeletal muscle atrophy. Physiol Res, 65:547-60.

114. Yamasaki R, Wu Y, McNabb M, Greaser M, Labeit S, Granzier H. (2002) Protein kinase A phosphorylates titin's cardiac-specific N2B domain and reduces passive tension in rat cardiac myocytes. Circ Res, 90:1181-8.

115. Koser F, Loescher C, Linke WA. (2019) Posttranslational modifications of titin from cardiac muscle: how, where, and what for? FEBS J, 286:2240-60.

116. Hidalgo C, Hudson B, Bogomolovas J, Zhu Y, Anderson B, Greaser M, Labeit S, Granzier H. (2009) PKC phosphorylation of titin's PEVK element: a novel and conserved pathway for modulating myocardial stiffness. Circ Res, 105:631-8, 17 p following 8.

117. Hidalgo C, Saripalli C, Granzier HL. (2014) Effect of exercise training on post-translational and post-transcriptional regulation of titin stiffness in striated muscle of wild type and IG KO mice. Arch Biochem Biophys, 552-553:100-7.

118. Kruger M, Kotter S, Grutzner A, Lang P, Andresen C, Redfield MM, Butt E, dos Remedios CG, Linke WA. (2009) Protein kinase G modulates human myocardial passive stiffness by phosphorylation of the titin springs. Circ Res, 104:87-94.

119. Hamdani N, Krysiak J, Kreusser MM, Neef S, Dos Remedios CG, Maier LS, Kruger M, Backs J, Linke WA. (2013) Crucial role for Ca2(+)/calmodulin-dependent protein kinase-II in regulating diastolic stress of normal and failing hearts via titin phosphorylation. Circ Res, 112:664-74.

120. Fukuda N, Wu Y, Nair P, Granzier HL. (2005) Phosphorylation of titin modulates passive stiffness of cardiac muscle in a titin isoform-dependent manner. J Gen Physiol, 125:257-71.

121. Perkin J, Slater R, Del Favero G, Lanzicher T, Hidalgo C, Anderson B, Smith JE, 3rd, Sbaizero O, Labeit S, Granzier H. (2015) Phosphorylating Titin's Cardiac N2B Element by ERK2 or CaMKIIdelta Lowers the Single Molecule and Cardiac Muscle Force. Biophys J, 109:2592-601.

122. Kruger M, Linke WA. (2006) Protein kinase-A phosphorylates titin in human heart muscle and reduces myofibrillar passive tension. J Muscle Res Cell Motil, 27:435-44.

123. Linke WA, Hamdani N. (2014) Gigantic business: titin properties and function through thick and thin. Circ Res, 114:1052-68.

124. Raskin A, Lange S, Banares K, Lyon RC, Zieseniss A, Lee LK, Yamazaki KG, Granzier HL, Gregorio CC, McCulloch AD, Omens JH, Sheikh F. (2012) A novel mechanism involving four-and-a-half LIM domain protein-1 and extracellular signal-regulated kinase-2 regulates titin phosphorylation and mechanics. J Biol Chem, 287:29273-84.

125. Muller AE, Kreiner M, Kotter S, Lassak P, Bloch W, Suhr F, Kruger M. (2014) Acute exercise modifies titin phosphorylation and increases cardiac myofilament stiffness. Front Physiol, 5:449.

126. Grutzner A, Garcia-Manyes S, Kotter S, Badilla CL, Fernandez JM, Linke WA. (2009) Modulation of titin-based stiffness by disulfide bonding in the cardiac titin N2-B unique sequence. Biophys J, 97:825-34.

127. Beckendorf L, Linke WA. (2015) Emerging importance of oxidative stress in regulating striated muscle elasticity. J Muscle Res Cell Motil, 36:25-36.

128. Kruger M, Kohl T, Linke WA. (2006) Developmental changes in passive stiffness and myofilament Ca2+ sensitivity due to titin and troponin-I isoform switching are not critically triggered by birth. Am J Physiol Heart Circ Physiol, 291:H496-506.

129. Opitz CA, Leake MC, Makarenko I, Benes V, Linke WA. (2004) Developmentally regulated switching of titin size alters myofibrillar stiffness in the perinatal heart. Circ Res, 94:967-75.

130. Chung CS, Hutchinson KR, Methawasin M, Saripalli C, Smith JE, 3rd, Hidalgo CG, Luo X, Labeit S, Guo C, Granzier HL. (2013) Shortening of the elastic tandem immunoglobulin segment of titin leads to diastolic dysfunction. Circulation, 128:19-28.

131. Chung CS, Hiske MA, Chadha A, Mueller PJ. (2020) Compliant Titin Isoform Content Is Reduced in Left Ventricles of Sedentary Versus Active Rats. Front Physiol, 11:15.

132. Dufrene YF, Ando T, Garcia R, Alsteens D, Martinez-Martin D, Engel A, Gerber C, Muller DJ. (2017) Imaging modes of atomic force microscopy for application in molecular and cell biology. Nat Nanotechnol, 12:295-307.

133. Kiss B, Mudra D, Torok G, Martonfalvi Z, Csik G, Herenyi L, Kellermayer M. (2020) Single-particle virology. Biophys Rev, 12:1141-54.

134. Martonfalvi Z, Kellermayer M. (2014) Individual globular domains and domain unfolding visualized in overstretched titin molecules with atomic force microscopy. PLoS One, 9:e85847.

135. de Pablo PJ, Schaap IAT. (2019) Atomic Force Microscopy of Viruses. Adv Exp Med Biol, 1215:159-79.

136. Rousso I, Deshpande A. (2022) Applications of Atomic Force Microscopy in HIV-1 Research. Viruses, 14.

137. Kiss B, Kis Z, Palyi B, Kellermayer MSZ. (2021) Topography, Spike Dynamics, and Nanomechanics of Individual Native SARS-CoV-2 Virions. Nano Lett, 21:2675-80.

138. Moreno-Herrero F, Perez M, Baro AM, Avila J. (2004) Characterization by atomic force microscopy of Alzheimer paired helical filaments under physiological conditions. Biophys J, 86:517-25.

139. Bouchonville N, Nicolas A. (2019) Quantification of the Elastic Properties of Soft and Sticky Materials Using AFM. Methods Mol Biol, 1886:281-90.

140. Li Y, Lang P, Linke WA. (2016) Titin stiffness modifies the force-generating region of muscle sarcomeres. Sci Rep, 6:24492.

141. Sziklai D, Sallai J, Papp Z, Kellermayer D, Martonfalvi Z, Pires RH, Kellermayer MSZ. (2022) Nanosurgical Manipulation of Titin and Its M-Complex. Nanomaterials (Basel), 12.

142. Weiner RB, Baggish AL. (2012) Exercise-induced cardiac remodeling. Prog Cardiovasc Dis, 54:380-6.

143. Mujika I, Padilla S. (2001) Cardiorespiratory and metabolic characteristics of detraining in humans. Med Sci Sports Exerc, 33:413-21.

144. Moker EA, Bateman LA, Kraus WE, Pescatello LS. (2014) The relationship between the blood pressure responses to exercise following training and detraining periods. PLoS One, 9:e105755.

145. Mujika I, Padilla S. (2000) Detraining: loss of training-induced physiological and performance adaptations. Part II: Long term insufficient training stimulus. Sports Med, 30:145-54.

146. Mujika I, Padilla S. (2000) Detraining: loss of training-induced physiological and performance adaptations. Part I: short term insufficient training stimulus. Sports Med, 30:79-87.

147. Ehsani AA, Hagberg JM, Hickson RC. (1978) Rapid changes in left ventricular dimensions and mass in response to physical conditioning and deconditioning. Am J Cardiol, 42:52-6.

148. Maron BJ, Pelliccia A, Spataro A, Granata M. (1993) Reduction in left ventricular wall thickness after deconditioning in highly trained Olympic athletes. Br Heart J, 69:125-8.

149. Banhegyi A, Pavlik G, Olexo Z. (1999) The effect of detraining on echocardiographic parameters due to injury. Acta Physiol Hung, 86:223-7.

150. Kemi OJ, Haram PM, Wisloff U, Ellingsen O. (2004) Aerobic fitness is associated with cardiomyocyte contractile capacity and endothelial function in exercise training and detraining. Circulation, 109:2897-904.

151. Pedlar CR, Brown MG, Shave RE, Otto JM, Drane A, Michaud-Finch J, Contursi M, Wasfy MM, Hutter A, Picard MH, Lewis GD, Baggish AL. (2018)

Cardiovascular response to prescribed detraining among recreational athletes. J Appl Physiol (1985), 124:813-20.

152. Mitchell AR, MacLachlan HI, Le Page P. (2013) Deconditioning the athletic heart. BMJ Case Rep, 2013.

153. Maron BJ, Pelliccia A, Spirito P. (1995) Cardiac disease in young trained athletes. Insights into methods for distinguishing athlete's heart from structural heart disease, with particular emphasis on hypertrophic cardiomyopathy. Circulation, 91:1596-601.

154. Pelliccia A, Maron BJ, Spataro A, Proschan MA, Spirito P. (1991) The upper limit of physiologic cardiac hypertrophy in highly trained elite athletes. N Engl J Med, 324:295-301.

155. Kubler J, Burgstahler C, Brendel JM, Gassenmaier S, Hagen F, Klingel K, Olthof SC, Blume K, Wolfarth B, Mueller KAL, Greulich S, Krumm P. (2021) Cardiac MRI findings to differentiate athlete's heart from hypertrophic (HCM), arrhythmogenic right ventricular (ARVC) and dilated (DCM) cardiomyopathy. Int J Cardiovasc Imaging.

156. Cunningham KS, Spears DA, Care M. (2019) Evaluation of cardiac hypertrophy in the setting of sudden cardiac death. Forensic Sci Res, 4:223-40.

157. Maron BJ, Thompson PD, Ackerman MJ, Balady G, Berger S, Cohen D, Dimeff R, Douglas PS, Glover DW, Hutter AM, Jr., Krauss MD, Maron MS, Mitten MJ, Roberts WO, Puffer JC, American Heart Association Council on Nutrition PA, Metabolism. (2007) Recommendations and considerations related to preparticipation screening for cardiovascular abnormalities in competitive athletes: 2007 update: a scientific statement from the American Heart Association Council on Nutrition, Physical Activity, and Metabolism: endorsed by the American College of Cardiology Foundation. Circulation, 115:1643-455.

158. Corrado D, Basso C, Rizzoli G, Schiavon M, Thiene G. (2003) Does sports activity enhance the risk of sudden death in adolescents and young adults? J Am Coll Cardiol, 42:1959-63.

159. Wang Y, Wisloff U, Kemi OJ. (2010) Animal models in the study of exercise-induced cardiac hypertrophy. Physiol Res, 59:633-44.

160. Hasenfuss G. (1998) Animal models of human cardiovascular disease, heart failure and hypertrophy. Cardiovasc Res, 39:60-76.

161. Wisloff U, Najjar SM, Ellingsen O, Haram PM, Swoap S, Al-Share Q, Fernstrom M, Rezaei K, Lee SJ, Koch LG, Britton SL. (2005) Cardiovascular risk factors emerge after artificial selection for low aerobic capacity. Science, 307:418-20.

162. Natali AJ, Turner DL, Harrison SM, White E. (2001) Regional effects of voluntary exercise on cell size and contraction-frequency responses in rat cardiac myocytes. J Exp Biol, 204:1191-9.

163. Kemi OJ, Loennechen JP, Wisloff U, Ellingsen O. (2002) Intensity-controlled treadmill running in mice: cardiac and skeletal muscle hypertrophy. J Appl Physiol (1985), 93:1301-9.

164. Wisloff U, Helgerud J, Kemi OJ, Ellingsen O. (2001) Intensity-controlled treadmill running in rats: VO(2 max) and cardiac hypertrophy. Am J Physiol Heart Circ Physiol, 280:H1301-10.

165. Evangelista FS, Brum PC, Krieger JE. (2003) Duration-controlled swimming exercise training induces cardiac hypertrophy in mice. Braz J Med Biol Res, 36:1751-9.

166. Hinken AC, Korte FS, McDonald KS. (2006) Porcine cardiac myocyte power output is increased after chronic exercise training. J Appl Physiol (1985), 101:40-6.

167. Polyak A, Kui P, Morvay N, Lepran I, Agoston G, Varga A, Nagy N, Baczko I, Farkas A, Papp JG, Varro A, Farkas AS. (2018) Long-term endurance training-induced cardiac adaptation in new rabbit and dog animal models of the human athlete's heart. Rev Cardiovasc Med, 19:135-42.

168. Olah A, Kellermayer D, Matyas C, Nemeth BT, Lux A, Szabo L, Torok M, Ruppert M, Meltzer A, Sayour AA, Benke K, Hartyanszky I, Merkely B, Radovits T. (2017) Complete Reversion of Cardiac Functional Adaptation Induced by Exercise Training. Med Sci Sports Exerc, 49:420-9.

169. Pelliccia A, Sharma S, Gati S, Back M, Borjesson M, Caselli S, Collet JP, Corrado D, Drezner JA, Halle M, Hansen D, Heidbuchel H, Myers J, Niebauer J, Papadakis M, Piepoli MF, Prescott E, Roos-Hesselink JW, Graham Stuart A, Taylor RS, Thompson PD, Tiberi M, Vanhees L, Wilhelm M, Group ESCSD. (2021) 2020 ESC Guidelines on sports cardiology and exercise in patients with cardiovascular disease. Eur Heart J, 42:17-96.

170. Perk J, De Backer G, Gohlke H, Graham I, Reiner Z, Verschuren WM, Albus C, Benlian P, Boysen G, Cifkova R, Deaton C, Ebrahim S, Fisher M, Germano G, Hobbs R, Hoes A, Karadeniz S, Mezzani A, Prescott E, Ryden L, Scherer M, Syvanne M, Op Reimer WJ, Vrints C, Wood D, Zamorano JL, Zannad F, European Association for Cardiovascular P, Rehabilitation. (2012) European guidelines on cardiovascular disease prevention in clinical practice (version 2012) : the fifth joint task force of the European society of cardiology and other societies on cardiovascular disease prevention in clinical practice (constituted by representatives of nine societies and by invited experts). Int J Behav Med, 19:403-88.

171. Olah A, Barta BA, Sayour AA, Ruppert M, Virag-Tulassay E, Novak J, Varga ZV, Ferdinandy P, Merkely B, Radovits T. (2021) Balanced Intense Exercise Training Induces Atrial Oxidative Stress Counterbalanced by the Antioxidant System and Atrial Hypertrophy That Is Not Associated with Pathological Remodeling or Arrhythmogenicity. Antioxidants (Basel), 10.

172. Czimbalmos C, Csecs I, Dohy Z, Toth A, Suhai FI, Mussigbrodt A, Kiss O, Geller L, Merkely B, Vago H. (2019) Cardiac magnetic resonance based deformation imaging: role of feature tracking in athletes with suspected arrhythmogenic right ventricular cardiomyopathy. Int J Cardiovasc Imaging, 35:529-38.

173. Fabian A, Ujvari A, Tokodi M, Lakatos BK, Kiss O, Babity M, Zamodics M, Sydo N, Csulak E, Vago H, Szabo L, Kiss AR, Szucs A, Merkely B, Kovacs A. (2022) Biventricular mechanical pattern of the athlete's heart: comprehensive characterization using 3D echocardiography. Eur J Prev Cardiol.

174. Coronado M, Fajardo G, Nguyen K, Zhao M, Kooiker K, Jung G, Hu DQ, Reddy S, Sandoval E, Stotland A, Gottlieb RA, Bernstein D. (2018) Physiological

Mitochondrial Fragmentation Is a Normal Cardiac Adaptation to Increased Energy Demand. Circ Res, 122:282-95.

175. Hudson B, Hidalgo C, Saripalli C, Granzier H. (2011) Hyperphosphorylation of mouse cardiac titin contributes to transverse aortic constriction-induced diastolic dysfunction. Circ Res, 109:858-66.

176. Knight PJ, Trinick JA. (1982) Preparation of myofibrils. Methods Enzymol, 85 Pt B:9-12.

177. Vikhorev PG, Ferenczi MA, Marston SB. (2016) Instrumentation to study myofibril mechanics from static to artificial simulations of cardiac cycle. MethodsX, 3:156-70.

178. Kellermayer MSZ, Voros Z, Csik G, Herenyi L. (2018) Forced phage uncorking: viral DNA ejection triggered by a mechanically sensitive switch. Nanoscale, 10:1898-904.

179. Hutter JL, Bechhoefer, J. (1993) Calibration of atomic-force microscope tips. Rev Sci Instrum, 64:1868-73.

180. Kellermayer MS, Smith SB, Granzier HL, Bustamante C. (1997) Folding-unfolding transitions in single titin molecules characterized with laser tweezers. Science, 276:1112-6.

181. Park SY, Gifford JR, Andtbacka RH, Trinity JD, Hyngstrom JR, Garten RS, Diakos NA, Ives SJ, Dela F, Larsen S, Drakos S, Richardson RS. (2014) Cardiac, skeletal, and smooth muscle mitochondrial respiration: are all mitochondria created equal? Am J Physiol Heart Circ Physiol, 307:H346-52.

182. Ogneva IV, Lebedev DV, Shenkman BS. (2010) Transversal stiffness and Young's modulus of single fibers from rat soleus muscle probed by atomic force microscopy. Biophys J, 98:418-24.

183. Akiyama N, Ohnuki Y, Kunioka Y, Saeki Y, Yamada T. (2006) Transverse stiffness of myofibrils of skeletal and cardiac muscles studied by atomic force microscopy. J Physiol Sci, 56:145-51.

184. Guasch E, Benito B, Qi X, Cifelli C, Naud P, Shi Y, Mighiu A, Tardif JC, Tadevosyan A, Chen Y, Gillis MA, Iwasaki YK, Dobrev D, Mont L, Heximer S, Nattel S. (2013) Atrial fibrillation promotion by endurance exercise: demonstration and mechanistic exploration in an animal model. J Am Coll Cardiol, 62:68-77.

185. Waring CD, Henning BJ, Smith AJ, Nadal-Ginard B, Torella D, Ellison GM. (2015) Cardiac adaptations from 4 weeks of intensity-controlled vigorous exercise are lost after a similar period of detraining. Physiol Rep, 3.

186. Guasch E, Mont L, Sitges M. (2018) Mechanisms of atrial fibrillation in athletes: what we know and what we do not know. Neth Heart J, 26:133-45.

187. Malek LA, Bucciarelli-Ducci C. (2020) Myocardial fibrosis in athletes-Current perspective. Clin Cardiol, 43:882-8.

188. D'Souza A, Bucchi A, Johnsen AB, Logantha SJ, Monfredi O, Yanni J, Prehar S, Hart G, Cartwright E, Wisloff U, Dobryznski H, DiFrancesco D, Morris GM, Boyett MR. (2014) Exercise training reduces resting heart rate via downregulation of the funny channel HCN4. Nat Commun, 5:3775.

189. Evangelista FS, Martuchi SE, Negrao CE, Brum PC. (2005) Loss of resting bradycardia with detraining is associated with intrinsic heart rate changes. Braz J Med Biol Res, 38:1141-6.

190. Scharhag J, Schneider G, Urhausen A, Rochette V, Kramann B, Kindermann W. (2002) Athlete's heart: right and left ventricular mass and function in male endurance athletes and untrained individuals determined by magnetic resonance imaging. J Am Coll Cardiol, 40:1856-63.

191. Martin WH, 3rd, Coyle EF, Bloomfield SA, Ehsani AA. (1986) Effects of physical deconditioning after intense endurance training on left ventricular dimensions and stroke volume. J Am Coll Cardiol, 7:982-9.

192. Pelliccia A, Maron MS, Maron BJ. (2012) Assessment of left ventricular hypertrophy in a trained athlete: differential diagnosis of physiologic athlete's heart from pathologic hypertrophy. Prog Cardiovasc Dis, 54:387-96.

193. Zhong L, Ghista DN, Ng EY, Lim ST. (2005) Passive and active ventricular elastances of the left ventricle. Biomed Eng Online, 4:10.

194. Chemla D, Coirault C, Hebert JL, Lecarpentier Y. (2000) Mechanics of Relaxation of the Human Heart. News Physiol Sci, 15:78-83.

195. Olah A, Nemeth BT, Matyas C, Hidi L, Lux A, Ruppert M, Kellermayer D, Sayour AA, Szabo L, Torok M, Meltzer A, Geller L, Merkely B, Radovits T. (2016) Physiological and pathological left ventricular hypertrophy of comparable degree is associated with characteristic differences of in vivo hemodynamics. Am J Physiol Heart Circ Physiol, 310:H587-97.

196. Obert P, Mandigout S, Vinet A, N'Guyen LD, Stecken F, Courteix D. (2001) Effect of aerobic training and detraining on left ventricular dimensions and diastolic function in prepubertal boys and girls. Int J Sports Med, 22:90-6.

197. Arany Z, He H, Lin J, Hoyer K, Handschin C, Toka O, Ahmad F, Matsui T, Chin S, Wu PH, Rybkin, II, Shelton JM, Manieri M, Cinti S, Schoen FJ, Bassel-Duby R, Rosenzweig A, Ingwall JS, Spiegelman BM. (2005) Transcriptional coactivator PGC-1 alpha controls the energy state and contractile function of cardiac muscle. Cell Metab, 1:259-71.

198. Suga H. (1990) Cardiac mechanics and energetics--from Emax to PVA. Front Med Biol Eng, 2:3-22.

8. Bibliography of the canidate's publications

8.1. Publications related to the PhD thesis

Oláh A*, **Kellermayer D***, Mátyás C, Németh BT, Lux Á, Szabó L, Török M, Ruppert M, Meltzer A, Sayour AA, Benke K, Hartyánszky I, Merkely B*, Radovits T*. (2017)
Complete Reversion of Cardiac Functional Adaptation Induced by Exercise Training. Med Sci Sports Exerc, 49: 420-429.
IF: 4.291
*: equal contribution

Kellermayer D, Kiss B, Tordai H, Oláh A, Granzier HL, Merkely B, Kellermayer M*, Radovits T*. (2021)
Increased Expression of N2BA Titin Corresponds to More Compliant Myofibrils in Athlete's Heart. Int J Mol Sci, 22: 11110.
IF: 6.208
*: equal contribution

Kellermayer D, Kiss B, Mártonfalvi Z, Radovits T, Merkely B, Kellermayer M.
Az izomrugalmasság óriásfehérjéje, a titin. (2020)
Magyar Sporttudományi Szemle, 83: 3-12.
IF:-

8.2. Publications not related to the PhD thesis

Radovits T, Oláh A, Lux Á, Németh BT, Hidi L, Birtalan E, **Kellermayer D**, Mátyás C, Szabó G, Merkely B. (2013)
Rat model of exercise-induced cardiac hypertrophy – hemodynamic characterization using left ventricular pressure-volume analysis. Am J Physiol Heart Circ Physiol, 305: H124-34
IF: 4.012

Oláh A, Németh BT, Mátyás C, Horváth EM, Hidi L, Birtalan E, **Kellermayer D,** Ruppert M, Merkely G, Szabó G, Merkely B, Radovits T. (2015)

Cardiac effects of acute exhaustive exercise in a rat model. Int J Cardiol, 182: 258-66.
IF: 4.638

Kovács A, Oláh A, Lux Á, Mátyás C, Németh BT, **Kellermayer D**, Ruppert M, Török M, Szabó L, Meltzer A, Assabiny A, Birtalan E, Merkely B, Radovits T. (2015)
Strain and strain rate by speckle tracking echocardiography correlate with pressure-volume loop derived contractility indices in a rat model of athlete's heart. Am J Physiol Heart Circ Physiol, 308: H743-8.
IF: 3.324

Mátyás C, Németh BT, Oláh A, Hidi L, Birtalan E, **Kellermayer D**, Ruppert M, Korkmaz S, Kökény G, Horváth EM, Szabó G, Merkely B, Radovits T. (2015)
The soluble guanylate cyclase activator cinaciguat prevents cardiac dysfunction in a rat model of type-1 diabetes mellitus. Cardiovasc Diabetol, 14: 145.
IF: 4.534

Oláh A, Németh BT, Mátyás C, Hidi L, Lux Á, Ruppert M, **Kellermayer D**, Sayour AA, Szabó L, Török M, Meltzer A, Gellér L, Merkely B, Radovits T. (2016)
Physiological and pathological left ventricular hypertrophy of comparable degree is associated with characteristic differences of in vivo hemodynamics. Am J Physiol Heart Circ Physiol, 310: H587-97.
IF: 3.348

Németh BT, Mátyás C, Oláh A, Lux Á, Hidi L, Ruppert M, **Kellermayer D**, Kökény G, Szabó G, Merkely B, Radovits T. (2016)
Cinaciguat prevents the development of pathologic hypertrophy in a rat model of left ventricular pressure overload. Sci Rep, 6: 37166
IF: 4.259

Mátyás C, Németh BT, Oláh A, Török M, Ruppert M, **Kellermayer D**, Barta BA, Szabó G, Kökény G, Horváth EM, Bódi B, Papp Z, Merkely B, Radovits T. (2017)

Prevention of the development of heart failure with preserved ejection fraction by the phosphodiesterase-5A inhibitor vardenafil in rats with type 2 diabetes. Eur J Heart Fail, 19: 326-336.
IF: 10.683

Kellermayer D, Smith JE 3rd, Granzier H. (2017)
Novex-3, the tiny titin of muscle. Biophys Rev, 9: 201-206.
IF: -

Oláh A, Kovács A, Lux Á, Tokodi M, Braun S, Lakatos BK, Mátyás C, **Kellermayer D**, Ruppert M, Sayour AA, Barta BA, Merkely B, Radovits T. (2019)
Characterization of the Dynamic Changes in Left Ventricular Morphology and Function Induced by Exercise Training and Detraining. Int J Cardiol, 277:178-185.
IF: 3.229

Kellermayer D, Smith JE 3rd, Granzier H. (2019)
Titin Mutations and Muscle Disease. Pflugers Arch, 471: 673-682.
IF: 3.158

Oláh A, Mátyás C, **Kellermayer D**, Ruppert M, Barta BA, Sayour AA, Török M, Koncsos G, Giricz Z, Ferdinandy P, Merkely B, Radovits T. (2019)
Sex Differences in Morphological and Functional Aspects of Exercise-Induced Cardiac Hypertrophy in a Rat Model. Front Physiol, 10: 889.
IF: 3.367

Sziklai D, Sallai J, Papp Z, **Kellermayer D**, Mártonfalvi Z, Pires RH, Kellermayer MSZ. (2022) Nanosurgical Manipulation of Titin and Its M-Complex. Nanomaterials (Basel), 12: 178.
IF: 5.719

DOI:10.14753/SE.2022.2759

9. Acknowledgements

I would like to say a special thank you to my tutor, Dr. Tamás Radovits for his enthusiasm and for providing guidance, feedback and continous support throughout my PhD studies. Without his invaluable knowledge and expertise in cardiovascular research this work would not have been possible.

I would like to thank Prof. Dr. Béla Merkely and Dr. Violetta Kékesi for providing excellent facilities and equipment and for their recommendations during the years of my PhD work.

I am grateful to Dr. Attila Oláh for his guidance and support during my scientific work. I would also like to thank Dr. Csaba Mátyás, Dr. Balázs Tamás Németh, Dr. Mihály Ruppert and Dr. Alex Ali Sayour for project discussions and suggestions. I would like to acknowledge Henriett Biró for the perfect technical assistance. In addition, I thank Dr. Henk Granzier for the collaboration studies.

I am truly greatful to Dr. Hedvig Tordai, Bálint Kiss and Krisztina Szendefyné Lór for their enduring support and much appreciated advice througout my research projects.

I would also like to extend my special thanks to my parents who inspire me along the unpredictable path of life. I would like to thank my father, Prof. Dr. Miklós Kellermayer for his commitment to conduct honest and meaningful scientific research and who provided constant technical and emotional support and guidance throughout my projects. Furthermore, I would like to thank my mother, Dr. Gyöngyi Szántó for her continuous support and encouragement throughout my scientific work and for always helping taking care of her granddaughter.

I am immensely thankful for the support, love and patience of my husband, András and our daughter, Sára. Without their encouragement, I would have not been able to conduct my scientific work.